Andean uplift, drainage basin formation, and the evolution of riverweeds *(Marathrum,* Podostemaceae*)* in northern South America

Ana M. Bedoya, Adam D. Leaché and Richard G. Olmstead
Department of Biology and Burke Museum, University of Washington, Seattle, WA, United States

Author for correspondence:
Ana M. Bedoya
Tel: +1 2063104972
Email: ambedoya@uw.edu

Summary

- Northern South America is a geologically dynamic and species-rich region. While fossil and stratigraphic data show that reconfiguration of river drainages resulted from mountain uplift in the tropical Andes, investigations of the impact of landscape change on the evolution of the flora in the region have been restricted to terrestrial taxa.
- We explore the role of landscape change on the evolution of plants living strictly in rivers across drainage basins in northern South America by conducting population structure, phylogenomic, phylogenetic networks, and divergence-dating analyses for populations of riverweeds (*Marathrum*, Podostemaceae).
- We show that mountain uplift and drainage basin formation isolated populations of *Marathrum* and created barriers to gene flow across rivers drainages. Sympatric species hybridize and the hybrids show the phenotype of one parental line. We propose that the pattern of divergence of populations reflect the formation of river drainages, which was not complete until <4 Ma
- Our study provides a clear picture of the role of landscape change in shaping the evolution of riverweeds in northern South America, advances our understanding of the reproductive biology of this remarkable group of plants, and spotlights the impact of hybridization in phylogenetic inference.

Key words: Andean uplift, Marathrum, next-generation sequencing, northern South America, phylogenomics, rivers, target enrichment

Introduction

Landscape change has been recognized as a major driver of diversification of lineages (Hoorn *et al.*, 2013). In the Neotropics, the most species-rich region in the world, the uplift of the Andean Cordillera is thought to have contributed directly and indirectly to the assembly of the terrestrial biota (Janzen, 1967; Kattan *et al.*, 2004; Antonelli & Sanmartín, 2011; Sklenář *et al.*, 2011; Smith *et al.*, 2014; Hoorn *et al.*, 2018; Quintero & Jetz, 2018). However, by shifting the physical locations of watershed boundaries, connecting and disconnecting adjacent river basins, (Albert & Crampton, 2010; Hoorn *et al.*, 2010; Tagliacollo *et al.*, 2015; Ruokolainen *et al.*, 2019) the uplift of the Andean Cordillera has also impacted the evolution of organisms living in rivers as has been shown in fish (Albert *et al.*, 2006, 2020; Picq *et al.*, 2014; Tagliacollo *et al.*, 2015). The role of Andean uplift in Neotropical plant evolution has been investigated in terrestrial groups living in mountains (Richardson *et al.*, 2018), where a correlation of Andean orogeny with increased diversification rates (Lagomarsino *et al.*, 2016; Pérez-Escobar *et al.*, 2017; Testo *et al.*, 2019), and explosive radiation in taxa in high-elevation tropical ecosystems (Hughes & Eastwood, 2006; Madriñán *et al.*, 2013; Nürk *et al.*, 2013; Nevado *et al.*, 2018) have been inferred. However, the impact of Andean uplift and landscape change in the region on plants in rivers remains unaddressed.

Here, we investigate the role of drainage basin formation linked to Andean uplift in shaping the evolution of river plants using riverweeds in the genus *Marathrum* (Podostemaceae) as a model system. Unlike most other angiosperms, except for the Hydrostachyaceae which are restricted to Africa and Madagascar, riverweeds are herbs that live attached to rocks partially or completely submerged in fast-flowing water ecosystems like river-rapids and waterfalls (Fig. **1b**) (van Royen, 1951; Philbrick & Novelo, 1995). The family has a Pantropical distribution and is the only group of aquatic plants in the Neotropics to live strictly in rivers (van Royen, 1951; Tippery *et al.*, 2011). Riverweeds are mostly annuals with short generation times and have flowers with a reduced perianth and capsular fruits that are produced and project above the water surface in the dry season (Willis, 1915; Philbrick & Novelo, 1998; Koi *et al.*, 2015). Hundreds of seeds are shed prior to the onset of the wet season when the water level is still low, and attach to the rock with a sticky mucilage (Reyes-Ortega *et al.*, 2009). The adult plants remain vegetative and attached to rocks via adhesive hairs and a biofilm of cyanobacteria (Rutishauser *et al.*, 1999; Jäger-Zürn & Grubert, 2000). Therefore, it has been suggested that the Podostemaceae have a reduced dispersal ability and are highly endemic (Philbrick *et al.*, 2010).

Within the Podostemaceae, the genus *Marathrum* has 22 recognized species (van Royen, 1951; Novelo & Philbrick, 1997; Novelo *et al.*, 2009; Tippery *et al.*, 2011). The genus is distributed in the West Indies,

Central America, and across the Andes in northern South America (nSA) (van Royen, 1951), making it the ideal model system for this study. The taxonomic classification of the group is confounded by the high degree of modification of vegetative organs (Rutishauser, 1995, 1997; Rutishauser *et al.*, 1999), as well as the reduced number of reproductive characters useful for classification (Philbrick, pers. comm.), which has resulted in multiple species proposed to be synonyms (Novelo *et al.*, 2009; Tippery *et al.*, 2011). Two species in particular are distinct from one another in their leaf type; *Marathrum utile* Tul. is the only species in the group with entire, laminar leaves (Fig. **1b**) (van Royen, 1951), whereas *Marathrum foeniculaceum* Bonpl. has highly dissected leaves (Fig. **1b**) and includes several other recognized species that have been proposed to be synonyms to it (Novelo *et al.*, 2009; Tippery *et al.*, 2011).

Palynological, stratigraphic, and macrofossil data (Latrubesse *et al.*, 2010; Hoorn *et al.*, 2010) support a landscape evolution model where from the Late Miocene (*ca.* 11Ma) to present, exceptionally rapid uplift of the Andes transformed the aquatic ecosystems in the region by causing a shift from a wetland-dominated environment, *Pebas Lake*, to the formation of current drainage basins interrupted by the Andes (*i.e.* Pacific, Magdalena, Orinoco, and Amazon; Fig. **1a**. Important features in the landscape of nSA include the Andean Cordillera, which in the region is divided into three ranges, *i.e.* the Western Cordillera (WC), Central Cordillera (CC), and Eastern Cordillera (EC) (Fig. **1a**). Another important topographic element is the Sierra Nevada de Santa Marta (SNSM) (Fig. **1a**), which is a separate formation from the Andes and is the highest coastal relief on earth (Duque-Caro, 1979; Villagómez *et al.*, 2011; Parra *et al.*, 2019). Multiple rivers originate in the SNSM (Fig. **1b**), with evidence for rapid and recent uplift of this mountain system (Villagómez *et al.*, 2011; Parra *et al.*, 2019). The rivers on the southern slopes of the SNSM are part of the Magdalena drainage basin (Abell *et al.*, 2008). However, these rivers are not connected through fast-flowing water currents to the other tributaries of the Magdalena drainage basin.

Given the dynamic nature of the landscape in northern South America and its role in shaping rivers, in this study we investigate how landscape change shaped the evolution of *Marathrum* in the region. We generate target enrichment and ddRADseq data and infer the genetic constitution of populations of *Marathrum* located across the Andes and the SNSM. We determine if there is gene flow across drainage basins and reconstruct the evolutionary relationships of populations of *Marathrum* using data concatenation, species tree, and phylogenetic network approaches. Using a species tree and a time-calibrated tree, we provide a hypothesis for the pattern and timing of divergence of populations of *Marathrum* currently disconnected by the Andes, the SNSM, and inter-Andean valleys. We propose that this pattern reflects the evolution of drainage basins in northern South America. Furthermore, this study

100 provides an insight into the reproductive biology of *Marathrum* and shows that hybridization confounds
101 phylogenetic inference of its populations.
102

103 **Materials and Methods**

104 Data collection, library preparation and sequencing

105 We collected 118 individuals; 115 of *Marathrum* (75 individuals of *M. foeniculaceum* and 40 individuals
106 of *M. utile*. See Fig. **1b**) and three of *Weddellina squamulosa* Tul. from Antioquia, (eastern slope of the
107 CC), Boyacá (eastern slope of the EC), and Caribe (SNSM) (Fig. **1a**). These populations are currently
108 disconnected by the Andes, the SNSM, inter-Andean valleys, and the lowlands between the Andes and
109 the SNSM (Fig. **1a**). Samples were preserved as vouchers, and tissues were taken from leaf material and
110 stored in silica gel. Voucher information is shown in Table S1. We extracted DNA from silica-dried leaf
111 material using a modified CTAB protocol (Doyle & Doyle, 1987) and purified the DNA extracts with
112 isopropanol precipitation. We assessed DNA concentration using a Qubit fluorometer and DNA
113 fragmentation levels using gel electrophoresis (1% agarose gels).
114

115 *Double digest Restriction Associated DNA sequencing (ddRADseq)*

116 We prepared ddRADseq libraries for 115 samples following the protocol described by Peterson *et al.*,
117 2012. In brief, we used *PstI* and *MspI* to double digest *ca.* 500 ng high-molecular DNA and purified
118 fragments with Sera-Mag SpeedBeads prior to ligation of barcoded Illumina adapters. Libraries were size
119 selected to 415–515 bp on a Pippin prep (Sage Science) using a modified protocol where pooled samples
120 were each run in a separate lane and size selected in reference to one lane running only the R2 marker
121 reagent. Final library amplification used Illumina indexed primers and HF-Phusion TAQ. We determined
122 library size distributions and concentrations on an Agilent 2200 TapeStation. Samples were sent to the
123 QB3 sequencing facility at UC Berkeley, where qPCR was performed to determine sequenceable library
124 concentrations prior to multiplexing equimolar amounts of each library and sequencing 150 single-end
125 reads in two lanes of an Illumina HiSeq 4000.
126

127 *Low-depth reference genome of Marathrum*

128 To identify single-copy orthologs for phylogenomic analyses, we collected genome-skimming data for
129 one individual of *Marathrum utile* (Table S1) generated at the QB3 sequencing facility (Berkeley, CA).
130 Total DNA was sheared to a target size of 300–500 bp and 150 paired-end reads were sequenced in an
131 Illumina HiSeq 4000. In order to select a set of target sequences that are nuclear, single-copy, and have
132 orthologs across *Marathrum*, we applied the methods in Chau *et al.*, 2018. Briefly, the *de novo* assembled

133 genome of *Marathrum utile*, a transcriptome of *Hypericum perforatum* L. (Hypericaceae) (assembly
134 generated by the 1kp project, sample code No. BNDE) (One Thousand Plant Transcriptomes Initiative,
135 2019; Carpenter *et al.*, 2019), a plastome of *Garcinia mangostana* L. (Calophyllaceae), and a
136 mitochondriome of *Populus tremula* L. (Salicaceae) (see Table S1 for sample information and accession
137 numbers) were used as input for the pipeline Sondovac (Schmickl et al., 2016). Sondovac removes reads
138 that map to the plastome or mitochondriome, and duplicated transcripts from the transcriptome and finds
139 genome reads matching the remaining unique transcripts, which are *de novo* assembled. The pipeline
140 filters the targets by length (minimum 600 bp for all contigs for a transcript, and 120 bp for each contig)
141 and uniqueness.
142
143 We complemented the set with the APVO SSC and pentatricopeptide repeat genes, which are shared
144 across angiosperms and have been found to be useful for resolution of inter-specific relationships in some
145 plant groups (Yuan et al., 2009, 2010; Duarte et al., 2010). The sequences were downloaded from
146 http://www.arabidopsis.org and used to conduct searches against the *M. utile* contigs in the draft genome
147 with BLASTN. Up to five of the top hits with a bit score >70 were retained. When hits for the same loci
148 overlapped from different contigs, we assembled the contigs using *de novo* assembly in Geneious v9.1.8.
149 We removed all hits matching the same locus with <95% pairwise identity as they could represent
150 paralogs. We retained individual sequences of at least 120 bp, and loci with at least 600 bp length.
151
152 *Target enrichment*
153 Taxon sampling for the target enrichment experiment was guided by a phylogenetic analysis of all the
154 ddRADseq data using SVDQuartets (Fig. S1) (Chifman & Kubatko, 2014). Of the 118 samples collected,
155 we selected 46 individuals for target enrichment with the aims of 1) including specimens with high-
156 quality genomic DNA and high coverage across the ddRADseq assembly, 2) sampling multiple
157 individuals per populations in each drainage basin, 3) providing equal representation of the clades
158 identified by the ddRADseq data. Probe design and sequencing were performed by RapidGenomics
159 (Gainesville, Florida, US). Briefly, 250–1000 ng of high-molecular DNA was fragmented to a target size
160 of 400 bp. Enriched pools were combined in equimolar ratios and probes were hybridized to pools to
161 enrich for targets. Probes targeting a loci space of 214,484 bp for 536 exons in 218 loci with 2x tiling
162 density were designed and 150 paired-end reads were sequenced in 25% of a lane of an Illumina HiSeq
163 3000. All raw sequence reads from the low-coverage genome, target enrichment experiment, and
164 ddRADseq datasets are deposited in the National Center for Biotechnology Information (NCBI) Sequence
165 Read Archive (Table S1).
166

Data processing:

ddRADseq

Following the exclusion of 20 samples that failed sequencing or had low coverage, ddRADseq data for the remaining 95 samples were quality checked with FastQC (https://www.bioinformatics.babraham.ac.uk/projects/fastqc/) and demultiplexed and assembled in ipyrad v0.9.42 (Eaton & Overcast, 2020) using a clustering threshold of 0.88. We removed consensus sequences that had low coverage (6 reads), excessive undetermined or heterozygous sites (>12), an excess of shared heterozygosity among samples (paralog filter=0.5), and included loci present in at least four individuals. Preliminary inspection of our resulting assemblies showed that there where high levels of missing data in our ddRADseq dataset with no loci recovered that are shared across ≥90% of the samples and only 70 loci shared across half of the samples (Table S2). In order to increase the number of shared loci across samples and allow for direct comparison of our two genomic datasets, we selected the ddRADseq samples that were also successfully sequenced in our target enrichment dataset (n=34). Reads from this subset where assembled in ipyrad v0.9.42 (Eaton & Overcast, 2020) with parameters specified as described above for the complete ddRADseq dataset, and we generated two alignments that included loci that were present in at least 17 individuals (*min17*; 50% missing data) and at least 4 individuals (*min4*; ~88% missing data).

Low-depth genome

Genome-skimming reads were loaded in FastQC to assess sequence quality. We used Trimmomatic v0.39 (Bolger *et al.*, 2014) to remove adapter sequences. *De novo* assembly was performed with the CLC Genomics Workbench 8 (https://digitalinsights.qiagen.com).

Target enrichment

We quality checked the demultiplexed target enrichment reads with FastQC and removed adapter sequences with Trimmomatic. Assembly of loci into genotypes with ambiguity codes may affect the accuracy of phylogenetic inference under the multispecies coalescent model (Andermann *et al.*, 2018). We assembled our target enrichment dataset in order to obtain alleles and not genotypes with ambiguity codes. Resulting paired and unpaired reads were assembled with the pipeline HybPiper to align, assemble mapped reads for each target sequence, and extract the coding sequence from the assembled contigs respectively. The best full-length contig is chosen by Hybpiper based on sequencing depth and percent identity with the reference sequence. Hence, for each individual, locus assembly with Hybpiper results in a single contig (allele) (Johnson *et al.*, 2016). Kates *et al.*, 2018 provided a framework for retrieving phased alleles from target enrichment data. However, the pipeline is appropriate for long-read data and

201 when used in our data, it yielded inaccurate assemblies. In this same study however, the authors
202 concluded that the effect of allele phasing compared to the use of random alleles as with Hybpiper is not
203 clear for phylogenetic reconstruction.
204 Assembled sequences for each sample were compiled, sorted by target sequence, and inspected for
205 paralogs using the scripts 'retrieve_sequences.py', and 'paralog_investigator.py'. Data on length of
206 assembled coding sequences for each target sequence and statistics on assembly efficiency were
207 calculated with the scripts 'get_seq_lengths.py' and 'hybpiper_stats.py'. Coding sequences with paralog
208 warnings were manually checked and potential paralogs were excluded from downstream analyses. Exons
209 that are in the same loci were concatenated and we used Geneious v9.1.8. (Biomatters Ltd., Auckland,
210 New Zealand) to create alignments for each loci with MAFFT v7.309 (Katoh & Standley, 2013), followed
211 by manual inspection.
212
213 Population structure across drainage basins
214 To examine population structure we ran ADMIXTURE v1.3 (Alexander *et al.*, 2009) and considered
215 clustering scenarios with up to 6 groups (K=1–6). SNPs used as input were extracted from our target
216 enrichment data with dDocent (Puritz *et al.*, 2014) by mapping the sequenced reads to the reference
217 sequences of our targeted loci, assembling the reads, and calling SNPs. We further filtered our resulting
218 SNPs to include loci with no missing data, only one SNP per locus, and a minor allele frequency of at
219 least 0.05 using VCFtools (Danecek *et al.*, 2011). Given the high degree of missing data in the ddRADseq
220 loci, we did not use these data for population structure inference.
221
222 Phylogenomics and phylogenetic networks
223 *Phylogenomics*
224 A total of 42 samples were successful in the target enrichment experiment (four *Marathrum* samples
225 failed sequencing or recovered relatively short exons of low quality. See Fig. S2), and these were used to
226 conduct phylogenetic inference using concatenated and coalescent approaches. The concatenated target
227 enrichment dataset and our *min17* ddRADseq assembly were analyzed under maximum likelihood (ML)
228 with RAxML-HPC BlackBox v8.2.12 (Stamatakis, 2014) on the CIPRES Science Gateway. We ran 1000
229 bootstrap replicates to assess branch support and considered each locus as a separate partition in our target
230 enrichment dataset. ddRADseq trees were rooted using the outgroup rooting of our target enrichment data
231 as a reference. Gene tree inference was conducted using the TICR pipeline (Stenz *et al.*, 2015) to run
232 MrBayes v3.2.7 (Ronquist & Huelsenbeck, 2003) for each target enrichment locus and generate 50%
233 consensus majority rule trees. We specified the GTR+G model of substitution (Abadi *et al.*, 2019) with 3
234 runs, 4 chains, 2 million generations, a sample frequency of 200, and a burn-in fraction of 0.25.

Species tree inference was conducted with ASTRAL III (Zhang *et al.*, 2018) and SVDQuartets (Chifman & Kubatko, 2014), both of which are coalescent-based approaches. Unrooted Bayesian gene trees were used as input for ASTRAL. We ran SVDQuartets analyses evaluating all quartets and using 1000 bootstraps on the concatenated sequences of our target capture data and the *min4* ddRADseq assembly. The latter comprises the maximum phylogenetic information necessary for a quartet based analysis (Eaton *et al.*, 2016) and is the data set that maximizes the number of shared loci recovered. The ddRADseq species trees were rooted using the outgroup rooting of our target enrichment data as a reference.

Phylogenetic networks

We explored non-bifurcating relationships in *Marathrum* by inferring phylogenetic networks in PhyloNet (Than *et al.*, 2008; Wen *et al.*, 2018). Following the results obtained with ADMIXTURE we randomly selected a subset of samples of *M. utile* and *M. foeniculaceum* from each drainage basin that did not show evidence of recent admixture. We kept those from Boyacá in order to infer how individuals in this population are related to Caribe and Antioquia. In addition, we conducted a second set of analyses that included admixed individuals expecting to find multiple reticulation events. For the latter, we created two datasets each of which included two individuals per population. We chose these individuals semi-randomly so that both "pure" and "admixed" individuals as inferred in ADMIXTURE were included. We rooted the previously inferred Bayesian consensus gene trees in R v4.0.2 with the outgroup *W. squamulosa* and inferred maximum pseudo-likelihood networks with 0–5 allowed reticulation events in PhyloNet. We followed Blair & Ané, 2020 in their recommendations for choosing among resulting phylogenetic networks by plotting the maximum number of allowed reticulations versus the resulting pseudolikelihood score, and selecting the number of reticulation events when a plateau begins to appear.

<u>Divergence times for populations across drainage basins</u>

To provide the evolutionary context in which populations of *Marathrum* diverged across drainage basins, we inferred a time tree with BEAST 2.6.0 (Bouckaert *et al.*, 2019). We run two chains for 3 billion generations. A secondary calibration was defined for the stem node of *Marathrum*, using *Weddellina squamulosa* as an outgroup and a broad normal prior distribution with a mean of 62 Ma and a standard deviation of 4 Ma. This distribution encompassed the results for this node reported in previous published work (Magallón *et al.*, 2015; Ruhfel *et al.*, 2016) that utilized the fossil *Paleoclusia chevalieri* Crepet & Nixon for calibration. We assessed convergence of runs with Tracer v1.7.1 (Rambaut *et al.*, 2018), discarded a 10% burnin fraction, combined the log files and posterior distribution of trees from the two

268 runs with LogCombiner, and generated a maximum clade credibility (MCC) tree with mean node heights
269 with TreeAnnotator.
270

271 **Results**

272 Data processing: ddRADseq, genome assembly, and target enrichment

273 The number of loci shared across samples in our complete data set (n=95) and ipyrad assembly statistics
274 for the subset of 34 samples (*min4* and *min17*) are in Tables S2 and S3. A total of 169,474 loci that are
275 shared in minimum 4 individuals were recovered across all 95 *Marathrum* and *Weddellina* samples, but
276 only 70 loci were recovered at 50% missing data) (Table S2). The *min4* (~88% missing data) and *min17*
277 (50% missing data) assemblies of our subset of 34 samples resulted in 28,023 and 679 recovered loci
278 respectively. Our results show that, although there are many loci recovered in our dataset, a smaller
279 proportion of those are present across most samples, with no loci shared in all of them.
280

281 *De novo* assembly of genome-skimming reads resulted in a draft assembled genome of *M. utile* consisting
282 of 627,733 contigs with a total length of 1.095 Gb and N50=11,454 bp (Bioproject PRJNA673497,
283 SRR12956182). After running the pipeline Sondovac using the draft genome as a template for the
284 identification of sequences to be targeted and applying our added filtering steps, we identified 536
285 sequences in 218 nuclear, single-copy loci. We recovered 208 loci across samples with an average of 507
286 exons in 205 loci. Figure S2 and Table S4 show the loci recovery efficiency and the number of sequences
287 and loci recovered per sample respectively. Recovery of assembled sequences was lower for the outgroup
288 taxa (*W. squamulosa*) but we included this sample for rooting purposes in downstream analyses.
289

290 Most warnings resulting from running paralog_investigator.py in Hybpiper corresponded to instances
291 where identical contigs that differed only in length were assembled to a target sequence for a sample. In
292 other instances, the differing contigs corresponded to alleles. In all such cases Hybpiper chooses the
293 contig with the highest coverage. When contigs have similar sequencing depth, Hybpiper chooses one
294 based on percent identity with the reference sequence (Johnson *et al.*, 2016). We excluded 28 exons
295 where multiple contigs mapped to the same reference sequence, contained more than two alleles per SNP
296 and included a high number of SNPs. By removing these exons, one locus was excluded.
297

298 Population structure across drainage basins

299 Read assembly and SNP calling in dDocent recovered 203 variant sites. Parametric population structure
300 estimation with ADMIXTURE resulted in a lower cross-validation error for *K*=4 and K=5 populations

301 (0.08310 and 0.09195, respectively; Fig. **2b** and Fig. S3). The best model shows that within each
302 Antioquia and Caribe there is strong population structure with two genetically distinct, non-admixed
303 clusters as well as multiple individuals with admixture proportions from the two clusters (*i.e.* hybrids). In
304 both drainage basins, the two distinct, non-admixed genetic clusters correspond to the phenotypes of *M.*
305 *foeniculaceum* and *M. utile*. All admixed individuals have about equal proportions of ancestry of the non-
306 admixed clusters. Furthermore, the admixed individuals have highly dissected leaves and their phenotype
307 corresponds to that of *M. foeniculaceum* (Fig. **1b**). There is no admixture detected in individuals of the
308 same species across drainage basins. The genetic constitution of the two individuals that represent the
309 population from Boyacá was inferred to include relatively equal proportions from *M. utile* from Caribe
310 and *M. foeniculaceum* from Antioquia. The only difference between K=4 and K=5 is that the latter detects
311 population substructure in *M. utile* from Antioquia.
312
313 <u>Phylogenomics and Phylogenetic networks</u>
314 *Phylogenomics*
315 Results from ML analyses of all samples with target enrichment and ddRADseq data are shown in Figs. **2**
316 and S4 respectively. Species trees for both datasets are shown in Fig. S5. Phylogenetic inference under
317 the species coalescent with SVDQuartets and ASTRAL III was performed using individuals as tips (See
318 Fig. S5) due to our prior evidence of the presence of admixed individuals **(Fig. 2b)**. The resulting trees do
319 not recover species as clades, contradicting the current taxonomic treatment of *Marathrum*, and
320 suggesting convergent evolution of forms in the genus. The target enrichment ML and ASTRAL III trees
321 (Figs. **2** and S5b) are consistent, with Antioquia and Boyacá forming sister clades, but differ in that *M.*
322 *utile* in Caribe is recovered as a clade in the species tree and as paraphyletic in the ML tree. Furthermore,
323 target enrichment trees (Figs. **2** and S5) show *M. foeniculaceum* and *M. utile* within each driange basin as
324 clades, except for the SVDQuartets tree (Fig. **2a**), where *M. foeniculaceum* from Antioquia is not
325 monophyletic. The placement of Boyacá differs in this tree as well. Unlike the target enrichment trees, the
326 trees inferred with ddRADseq data using ML (Fig. S4) and SVDQuartets (Fig. S5a) do not recover
327 individuals with the phenotypes of *M. foeniculaceum* or *M. utile* in Caribe as clades. The ddRADseq trees
328 differ in the placement of Boyacá and in the recovery of *M. foeniculaceum* from Antioquia as
329 paraphyletic and monophyletic in the ML and SVDQuartets trees respectively. The latter tree exhibits
330 weak support for most branches.
331
332 To explore and eliminate the conflict that can arise in phylogenetic reconstruction with the inclusion of
333 admixed individuals that have ancestry proportions from *M. foeniculaceum* and *M. utile* inhabiting the
334 same drainage basin, we removed all admixed individuals. However, we kept those from Boyacá in order

335 to infer how individuals in this population are related to Caribe and Antioquia. We re-analyzed our data as
336 described above, but we also conducted Bayesian inference (BI) in MrBayes v3.2.7 with 2 runs, 4 chains,
337 10 million generations, a sample frequency of 10,000, and a burn-in fraction of 0.25. Phylogenetic
338 inference with ddRADseq on concatenated data was inferred from an ipyrad assembly with ~50% missing
339 data, whereas species tree inference was conducted on an assembly with minimum four individuals per
340 loci (Table S3 for ipyrad statistics). Each locus in our target enrichment dataset was set as a separate
341 partition specifying the GTR+G substitution model for each partition (Abadi *et al.*, 2019). The GTR+G
342 substitution model was also specified in the BI analysis of ddRADseq. We used the recovered genetic
343 units from ADMIXTURE as the taxonomic units for species tree inference.
344
345 Results from these analyses are shown in Fig. **3**. These fundamentally contradict the results reported
346 above using admixed and non-admixed individuals together. Maximum likelihood and BI trees of target
347 enrichment data (Fig. **3a** and S6) and species trees for both datasets (Fig. **3b,c**) support the current
348 taxonomic treatment of *Marathrum,* with *M. foeniculaceum* recovered as monophyletic and *M. utile* either
349 as monophyletic (SVDQuartets inference in Fig. **3b**) or paraphyletic (ML, BI and ASTRAL III trees in
350 Fig. **3a,c**, and S6). Plants from Boyacá, all of which have the phenotype of *M. foeniculaceum* (Fig. **1**), are
351 found as sister to *M. foeniculaceum* from Antioquia and Caribe in all species tree inferences. Maximum
352 likelihood (Fig. S6) and BI (Fig. **3a**) analyses of ddRADseq, which as mentioned before is characterized
353 by high levels of missing data, show a biogeographic pattern where Antioquia evolves from Caribe and
354 do not recover *M. foeniculaceum* and *M. utile* as clades. The reasons for the discordance among target
355 enrichment and ddRADseq datasets are further discussed.
356
357 *Phylogenetic networks*
358 Comparison of pseudolikelihood scores for 0–5 maximum reticulation events show that at two allowed
359 reticulations, the change in pseudolikelihood begins to plateau (Fig. **4**). The phylogenetic network shows
360 a reticulation event in the branch that leads to the two individuals from Boyacá, in line with our
361 phylogenetic reconstructions excluding admixed individuals and our ADMIXTURE results. A second
362 reticulation event is inferred deeper in the phylogeny with *M. foeniculaceum* as either sister to *M. utile* or
363 originating from it. When including admixed individuals in our analysis, comparison of pseudolikelihood
364 scores show that after 5 reticulation events, the change in pseudolikelihood has not plateaued (Fig. S7),
365 suggesting that multiple admixture events have taken place in *Marathrum* in northern South America.
366

367 Divergence times for populations across drainage basins
368 The BEAST calibrated phylogeny of *Marathrum* is shown in Fig. **5**. All populations sampled across the
369 Andes and the SNSM are inferred to have shared a most recent common ancestor at ~4Ma at most. The
370 topology supports the current taxonomic treatment of the group and is consistent with our phylogenetic
371 trees obtained from target enrichment concatenated data and after excluding admixed individuals.
372 Divergence times obtained in our study are compared to previous studies where the crown age of
373 Podostemaceae was also estimated in Table 1.
374

375 **Discussion**
376 Together, our population structure, phylogenomic, phylogenetic networks, and divergence-dating
377 analyses inform us about how through the Miocene and Pliocene, landscape change in northern South
378 America shaped the evolution of *Marathrum* and of river basins. We show that during this time period,
379 populations of both *M. foeniculaceum* and *M. utile* split into different drainage basins currently
380 interrupted by the Andes, the SNSM, and inter-Andean valleys and became genetically distinct (Figs.
381 **3,5**). As a result, strong population structure consistent with geography was inferred in populations of
382 each species (Fig. **2**). At the same time we demonstrate that there is little to no gene flow in populations
383 of the same species across drainage basins (Fig. **2**) and therefore, that the Andean cordilleras, the SNSM,
384 and/or inter-Andean valleys currently act as barriers that limit gene flow in this particular group of plants.
385 We found that while populations across drainage basins became genetically distinct, the sympatric
386 distribution of *M. foeniculaceum* and *M. utile* resulted in hybridization within drainage basins, and we
387 report that hybrids show the phenotype of only *M. foeniculaceum*. The current taxonomic treatment of the
388 genus is validated in this study. Divergence dating results imply that fast-flowing water ecosystems in
389 Antioquia, Caribe, and Boyacá and populations of *Marathrum* inhabiting them became isolated (Fig. **5**)
390 very recently in geologic time (< 4Ma). We propose that the phylogenetic relationships of populations
391 (namely Boyacá as sister to Caribe-Antioquia) reflect the scenario for the divergence of drainage basins
392 as the Andes uplifted (Fig. **3**).
393

394 Population structure across drainage basins
395 *Barriers to gene flow*
396 In addition to mountains and valleys being a barrier to gene flow in populations of *M. foeniculaceum and*
397 *M. utile* in northern South America, a limited dispersal ability of pollen or seeds in these plants could
398 contribute to the strong population structure and lack of within species gene flow reported here across
399 drainage basins (Fig. **2**). This is in line with previous work on Podostemaceae, where high levels of

differentiation among populations of *Hydrobium japonicum* and *Cladopus doianus* in Japan and of *Podostemum irgangii* in Brazil were attributed to be the result of reduced dispersal due to their restricted habitat (Baggio *et al.*, 2013; Katayama *et al.*, 2016). This pattern is also seen in freshwater fishes (which share the same habitat as *Marathrum*) where range evolution is generally constrained by watershed boundaries (Albert & Crampton, 2010; Lujan & Armbruster, 2011; Musilová *et al.*, 2013; Picq *et al.*, 2014; Roxo *et al.*, 2014; Tagliacollo *et al.*, 2015; Lujan *et al.*, 2019; Albert *et al.*, 2020).

However, long-distance dispersal has been invoked as the explanation for the pantropical distribution of Podostemaceae (Kita & Kato, 2004; Koi *et al.*, 2015; Ruhfel *et al.*, 2016). Birds may be possible vectors for seed dispersal in Podostemaceae if seeds get attached to their feet via a sticky mucilage in the seed coat (Willis, 1902; Philbrick & Novelo, 1995, 1997; Leleeka *et al.*, 2016). Future work should focus on the extent of dispersal of Podostemaceae within a single river and across rivers to determine how seed and pollen dispersal is facilitated or hindered.

Genetic drift

Populations of *Marathrum* and of Podostemaceae in general tend to be small, with a discontinuous distribution due to their high degree of habitat specificity (Willis, 1914; van Royen, 1951; Rutishauser, 1995; Cook, 1996; Philbrick *et al.*, 2010; Koi *et al.*, 2015; Cheek & Lebbie, 2018). We believe that in such small populations with short generation times, genetic drift may be a rather strong evolutionary force. As drainage basins were established, this mechanism would have acted independently in populations of each species within each drainage basin, quickly fixing their alleles, and resulting in homogeneous populations that are genetically distinct across drainage basins as found in this study for *Marathrum* (Fig. **2**).

Hybridization scenarios and phenotype

Luna *et al.*, 2012 mentioned hybridization as a possible explanation for the existence of intermediate morphotypes among closely related species of *Marathrum* that are morphologically similar. In that same study however, the authors concluded that cross-compatibility is between morphological variants of the same species which had been previously synonymized under *M. foeniculaceum* (Novelo *et al.*, 2009; Tippery *et al.*, 2011). Our study includes key insights into the reproductive biology of *Marathrum* by providing clear genomic evidence for hybridization without introgression between two phenotypically and phylogenetically distinct species in *Marathrum.*

433 We propose two hypotheses for the uniformity in admixture proportions across admixed individuals in
434 Antioquia and Caribe (Fig. **2**). The genetic constitution of admixed individuals in these two drainage
435 basins stems from 1) very recent and frequent admixture events (*i.e*. F1 hybrids of the two species with no
436 further mixing or backcrossing) or 2) a past hybridization event followed by genome duplication resulting
437 in allopolyploids. Under the latter scenario, hybridization needs to have occurred at minimum once in
438 each river basin but not every generation. Fertile allopolyploids would reproduce the admixed genomes
439 (and the *M. foeniculaceum* morphotype). Variation in ploidy and cell DNA content are unknown for these
440 populations.
441
442 The dual ancestry of the two individuals that represent the population from Boyacá stems from *M. utile*
443 from Caribe and *M. foeniculaceum* from Antioquia in more or less equal proportions (Fig. **2**). No
444 individuals of *M. utile* and *M. foeniculaceum* are known to exist in or close to that population. Sampling
445 needs to be expanded to confirm this pattern in more individuals in Boyacá, and to test whether admixture
446 in individuals of this population is a result of recent hybridization with or without long distance transport
447 of pollen or seeds, retention of ancestral polymorphism in this population, or allopolyploidy.
448
449 This study spotlights an interesting case of inheritance of a phenotypic trait: leaf shape. Given that all
450 admixed individuals and putative hybrids show the phenotype of *M. foeniculaceum* (Figs. **1** and **2**), a
451 likely hypothesis is that leaf shape is controlled by one or few genes, with highly dissected leaves being
452 the dominant trait. Common garden experiments could test the hybrid origin of the admixed individuals
453 and the genetic basis of leaf morphology.
454
455 <u>Phylogenomics</u>
456 *Incongruence in ddRAdseq vs target enrichment datasets with concatenated data*
457 Missing data, internal short branches like those shown in our inferred trees in Figs. **2, 3a,** and S4 and
458 bioinformatic steps used for the assembly of loci (e.g. clustering threshold), have a strong impact on tree
459 inference (Leaché *et al.*, 2015). These three phenomena are characteristic of our ddRADseq data and may
460 be responsible for the discordance among datasets in this study (Figs. **3a** S5, and S6). As shown in Table
461 S3, our ddRADseq data are characterized by high levels of missing data, possibly as a result of previously
462 suggested high rates of evolution in Podostemaceae (Bedoya *et al.*, 2019). Rapid evolution would result
463 in high sequence divergence, and allelic dropout would reduce the number of shared loci recovered
464 (Wagner *et al.*, 2013; Arnold *et al.*, 2013; Eaton *et al.*, 2016). Incomplete lineage sorting (ILS) could be
465 responsible for the recovery of the two individuals from Boyacá as paraphyletic in the tree inferred from
466 the concatenated data using target enrichment data (Fig. **3a**), but more individuals should be sampled

467 from this population to support this claim. When ILS is accounted for with quartet analysis of our *min4*
468 ddRADseq data, phylogenetic inference is congruent with the trees inferred from target enrichment. The
469 latter trees are free from the biases mentioned above and therefore provide more reliable results for
470 discussing the evolutionary history of *Marathrum.*
471
472 *Systematics of Marathrum*
473 Our results demonstrate that *M. foeniculaceum* and *M. utile* are consistent with traditional taxonomic units
474 (Fig. **3**), being most likely both monophyletic as inferred with SVDQuartets, or an ancestor-descendant
475 species pair as resulting from ASTRAL III analyses. Even though both ASTRAL III and SVDQuartets
476 consider ILS as a source for gene tree incongruence, species tree inference may be inconsistent when
477 gene trees are estimated from data for loci of finite length (Wascher & Kubatko, 2020) as is the case in
478 ASTRAL III. In contrast, SVDQuartets has been confirmed to be statistically consistent under various
479 scenarios of ILS (Wascher & Kubatko, 2020). Our phylogenetic reconstructions are affected by the
480 inclusion of admixed individuals (Figs. **2**, **3,** and S4). This is because hybrids contain alleles originating
481 from both parents (Bastide *et al.*, 2018; Zhang *et al.*, 2019) causing the parental lineages and hybrids to
482 cluster together. This phenomenon has been reported across various groups (McVay *et al.*, 2017; García
483 *et al.*, 2017; Zhang *et al.*, 2019; Ginsberg *et al.*, 2019) and affects both concatenated and species tree
484 inference (Leaché *et al.*, 2014).
485
486 Landscape change, river basin formation and timing of divergence of populations of *Marathrum* in nSA
487 With the evidence presented above, we propose that the pattern of divergence of Antioquia, Boyacá, and
488 Caribe tracks the scenario in which drainage basins split from one another. Based on our species tree
489 inferences, Boyacá (eastern slope of the EC) diverged earlier from Caribe and Antioquia. Even though the
490 SVDQuartets species tree shows weak support for the placement of *M. foeniculaceum* from Boyacá, both
491 this and the ASTRAL III (Fig. **3b,c**) show the same biogeographic pattern. Reticulation events (Fig. **4**)
492 could have taken place in sympatry or be the result of vicariance followed by secondary contact mediated
493 by, for example, river capture events or less likely, long distance dispersal.
494
495 Several studies document that major pulses of uplift took place during the Late Miocene and Pliocene
496 asynchronously across the three Andean cordilleras at *ca.* 12–6 Ma and *ca.* 4.5 Ma, resulting in the
497 current elevation of the Andes (Gregory-Woodzicki, 2000; Garzione *et al.*, 2008; Mora *et al.*, 2010;
498 Hoorn *et al.*, 2010). These dates are contested by geological studies of mainly coarse-grained deposits that
499 suggest that the Eastern Cordillera was already well underway in Eocene times and nearly complete in the
500 Late Miocene (>11 Ma) (Cooper *et al.*, 1995; Montes *et al.*, 2019; Rodríguez-Muñoz *et al.*, 2020). Our

divergence dating analysis results in Fig. **5** imply that the orogenic history of the Andean Cordillera and inter-Andean valley formation proposed by either of the two hypotheses, did not result in the complete separation of the currently isolated, genetically distinct populations of *M. foeniculaceum* and *M. utile* in Antioquia, Boyacá and Caribe until < 5 Ma.

Furthermore, we favor the hypothesis of rapid pulses of Andean uplift in the Late Miocene and Pliocene by showing that the establishment of completely isolated fast-flowing water ecosystems in Antioquia, Caribe and Boyacá was not completed until < 4Ma (Fig. **5**) when the Andes, SNSM, and inter-Andean valleys became a barrier to gene flow. Our results are in line with Anderson *et al.*, 2016 who using U-Pb detrital zircon provenance, petrographic and paleoprecipitation data, conclude that the northern Andes was not a substantial orographic river barrier until *ca.* 3–6 Ma when rapid uplift took place. A lowland connection between the Amazon, Caribe and Magdalena drainage basins is corroborated by the affinity of fossils in Miocene and Pliocene deposits found across drainage basins (Lundberg & Chernoff, 1992; Aguilera *et al.*, 2013). The short branches and very recent splits in populations in Caribe indicate that the rivers in this drainage basin originated and split very recently in geologic time (Figs. **3, 5**, and S4). Indeed, surface uplift that gave rise to the current topology of the SNSM has been proposed to have taken place no earlier than 2 Ma (Villagómez *et al.*, 2011; Parra *et al.*, 2019).

Since our calibrated phylogeny was inferred from concatenated data, the dates inferred for each of the nodes could be more recent than if species tree inference was used instead. However, the joint inference of gene trees and a calibrated species tree in *BEAST is computationally intensive and feasible only for moderate-size datasets (McCormack *et al.*, 2013). Divide-and-conquer methods must be used to improve scalability in species tree estimation in *BEAST (Zimmermann *et al.*, 2014) if hundreds of loci are to be considered, potentially increasing the uncertainty in the estimation of node ages. This study represents a significant advance in our understanding of the impact of landscape change in the evolution of plants in rivers in northern South America and provides a comprehensive genomic dataset for the only plant genus that inhabits fast-flowing water ecosystems across the Western, Central, and Eastern Andean cordilleras and the Sierra Nevada de Santa Marta.

Acknowledgements

We are thankful to Dr. C.Thomas Philbrick for his helpful and thorough insights into the biology and classification of Podostemaceae, access to voucher specimens, and help with determination of samples. Special thanks to Dr. Santiago Madriñán at the Universidad de los Andes and the Jardín Botánico de Cartagena “Guillermo Piñeres”, Turbaco, Colombia for facilitating field work logistics and providing

facilities for specimen processing in Colombia. We thank Dr. Camilo Montes at the Universidad del Norte, Barranquilla, Colombia for insightful conversations on the geological background of nSA, and Dr. Camila Martínez at the Smithsonian Institution in Panama for comments on the manuscript. Maria Paula Contreras, David Ocampo, Daniel Ocampo, Jules Dominé, Fernando Bedoya, and Adrián Pinzón provided invaluable assistance in the field. Viviana Londoño provided a sample of *M. foeniculaceum*. Voucher specimens are deposited at the UNIANDES herbarium of the Universidad de los Andes, Bogota, Colombia. Samples were collected under the MARCO collecting permit Res. No. 1177 October 9, 2014 of the Universidad de los Andes. Funding was provided by the Botanical Society of America and American Society of Plant Taxonomists Research Awards, Explorers Club Exploration Fund Grant, Department of Biology at the University of Washington Giles Award and WRF Hall International Endowed Fellowship, UW Herbarium Endowment, UW Graduate School Boeing International Fellowship, and the Colciencias fellowship for Graduate studies (Doctorados en el Exterior-679) to A.M.B. This work used the Vincent J. Coates Genomics Sequencing Laboratory at UC Berkeley, supported by NIH S10 OD018174 Instrumentation Grant.

Author Contribution

A.M.B. and R.G.O designed the study. A.M.B. collected and analyzed the data; R.G.O. and A.D.L. provided guidance on the methods for data analyses and interpretation of results, as well as reagents, equipment, and laboratory space. A.M.B. wrote the manuscript with significant contributions from R.G.O and A.D.L.

Data Availability

All raw sequence reads from the low-coverage genome, target enrichment experiment, and ddRADseq datasets are deposited in the National Center for Biotechnology Information (NCBI) Sequence Read Archive under Bioproject PRJNA673497 (available upon initial acceptance). Fasta sequences of targeted loci, processed data and all trees generated in this study will be deposited in a public repository upon initial acceptance.

References

Abadi S, Azouri D, Pupko T, Mayrose I. **2019**. Model selection may not be a mandatory step for phylogeny reconstruction. *Nature Communications* **10**: 934.

Abell R, Thieme ML, Revenga C, Bryer M, Kottelat M, Bogutskaya N, Coad B, Mandrak N, Balderas SC, Bussing W, *et al.* 2008. Freshwater Ecoregions of the World: A New Map of Biogeographic Units for Freshwater Biodiversity Conservation. *BioScience* **58**: 403–414.

Aguilera O, Lundberg J, Birindelli J, Pérez MS, Jaramillo C, Sánchez-Villagra MR. **2013**. Paleontological evidence for the last temporal occurrence of the ancient Western Amazonian river outflow into the Caribbean. **8**: e76202.

Albert JS, Crampton WGR. **2010**. The geography and ecology of diversification in Neotropical freshwaters. **3**: 13.

Albert JS, Lovejoy NR, Crampton WGR. **2006**. Miocene tectonism and the separation of cis- and trans-Andean river basins: Evidence from Neotropical fishes. *Journal of South American Earth Sciences* **21**: 14–27.

Albert JS, Tagliacollo VA, Dagosta F. **2020**. Diversification of Neotropical Freshwater Fishes. *Annual Review of Ecology, Evolution, and Systematics* **51**: annurev-ecolsys-011620-031032.

Alexander DH, Novembre J, Lange K. **2009**. Fast model-based estimation of ancestry in unrelated individuals. *Genome Research* **19**: 1655–1664.

Andermann T, Fernandes AM, Olsson U, Töpel M, Pfeil B, Oxelman B, Aleixo A, Faircloth BC, Antonelli A. **2018**. Allele Phasing Greatly Improves the Phylogenetic Utility of Ultraconserved Elements (S Renner, Ed.). *Systematic Biology*.

Anderson VJ, Horton BK, Saylor JE, Mora A, Tesón E, Breecker DO, Ketcham RA. **2016**. Andean topographic growth and basement uplift in southern Colombia: Implications for the evolution of the Magdalena, Orinoco, and Amazon river systems. *Geosphere* **12**: 1235–1256.

Antonelli A, Sanmartín I. **2011**. Why are there so many plant species in the Neotropics? *TAXON* **60**: 403–414.

Arnold B, Corbett-Detig RB, Hartl D, Bomblies K. **2013**. RADseq underestimates diversity and introduces genealogical biases due to nonrandom haplotype sampling. *Molecular Ecology* **22**: 3179–3190.

Baggio RA, Firkowski CR, Boeger MRT, Boeger WA. **2013**. Differentiation within and between river basins of Podostemum irgangii (Podostemaceae), a rapid-water macrophyte of southern Brazil. *Aquatic Botany* **107**: 33–38.

Bastide P, Solís-Lemus C, Kriebel R, William Sparks K, Ané C. **2018**. Phylogenetic Comparative Methods on Phylogenetic Networks with Reticulations (F Burbrink, Ed.). *Systematic Biology* **67**: 800–820.

Bedoya AM, Ruhfel BR, Philbrick CT, Madriñán S, Bove CP, Mesterházy A, Olmstead RG. **2019**. Plastid Genomes of Five Species of Riverweeds (Podostemaceae): Structural Organization and Comparative Analysis in Malpighiales. *Frontiers in Plant Science* **10**: 1035.

Blair C, Ané C. **2020**. Phylogenetic Trees and Networks Can Serve as Powerful and Complementary Approaches for Analysis of Genomic Data (M Hahn, Ed.). *Systematic Biology* **69**: 593–601.

Bolger AM, Lohse M, Usadel B. **2014**. Trimmomatic: a flexible trimmer for Illumina sequence data. *Bioinformatics* **30**: 2114–2120.

Bouckaert R, Vaughan TG, Barido-Sottani J, Duchêne S, Fourment M, Gavryushkina A, Heled J, Jones G, Kühnert D, De Maio N, *et al.* 2019. BEAST 2.5: An advanced software platform for Bayesian evolutionary analysis (M Pertea, Ed.). *PLOS Computational Biology* **15**: e1006650.

Carpenter EJ, Matasci N, Ayyampalayam S, Wu S, Sun J, Yu J, Jimenez Vieira FR, Bowler C, Dorrell RG, Gitzendanner MA, *et al.* 2019. Access to RNA-sequencing data from 1,173 plant species: The 1000 Plant transcriptomes initiative (1KP). *GigaScience* **8**: giz126.

Chau JH, Rahfeldt WA, Olmstead RG. **2018**. Comparison of taxon-specific versus general locus sets for targeted sequence capture in plant phylogenomics. *Applications in Plant Sciences* **6**: e1032.

Cheek M, Lebbie A. **2018**. Lebbiea (Podostemaceae-Podostemoideae), a new, nearly extinct genus with foliose tepals, in Sierra Leone (A Hemp, Ed.). *PLOS ONE* **13**: e0203603.

Chifman J, Kubatko L. **2014**. Quartet Inference from SNP Data Under the Coalescent Model. *Bioinformatics* **30**: 3317–3324.

Cook CDK. **1996**. *Aquatic plant book*. The Hague, Netherlands: SPB Academic.

Cooper MA, Addison FT, Alvarez R, Coral M, Graham RH, Hayward AB, Howe S, Martinez J, Naar J, Peñas R, *et al.* 1995. Basin development and tectonic history of the Llanos basin, Eastern Cordillera, and Middle Magdalena Valley, Colombia. **79**: 1421–1442.

Danecek P, Auton A, Abecasis G, Albers CA, Banks E, DePristo MA, Handsaker RE, Lunter G, Marth GT, Sherry ST, *et al.* 2011. The variant call format and VCFtools. *Bioinformatics* **27**: 2156–2158.

De la Ossa-Guerra LE, Santos MH, Artoni RF. **2020**. Genetic Diversity of the Cichlid Andinoacara latifrons (Steindachner, 1878) as a Conservation Strategy in Different Colombian Basins. *Frontiers in Genetics* **11**: 815.

Doyle JJ, Doyle JL. **1987**. A rapid DNA isolation procedure for small quantities of fresh leaf tissue. **19**: 11–15.

Duarte JM, Wall PK, Edger PP, Landherr LL, Ma H, Pires JC, Leebens-Mack J, dePamphilis CW. **2010**. Identification of shared single copy nuclear genes in Arabidopsis, Populus, Vitis and Oryza and their phylogenetic utility across various taxonomic levels. *BMC Evolutionary Biology* **10**: 61.

Duque-Caro H. **1979**. Major structural elements and evolution of northwestern Colombia. In: Geological and geophysical investigations of continental margins: AAPG Memoir. 329–351.

Eaton DAR, Overcast I. **2020**. ipyrad: Interactive assembly and analysis of RADseq datasets (R Schwartz, Ed.). *Bioinformatics* **36**: 2592–2594.

Eaton DAR, Spriggs EL, Park B, Donoghue MJ. **2016**. Misconceptions on Missing Data in RAD-seq Phylogenetics with a Deep-scale Example from Flowering Plants. *Systematic Biology*: 399–412.

García N, Folk RA, Meerow AW, Chamala S, Gitzendanner MA, Oliveira RS de, Soltis DE, Soltis PS. **2017**. Deep reticulation and incomplete lineage sorting obscure the diploid phylogeny of rain-lilies and allies (Amaryllidaceae tribe Hippeastreae). *Molecular Phylogenetics and Evolution* **111**: 231–247.

Garzione CN, Hoke GD, Libarkin JC, Withers S, MacFadden B, Eiler J, Ghosh P, Mulch A. **2008**. Rise of the Andes. *Science* **320**: 1304–1307.

Ginsberg PS, Humphreys DP, Dyer KA. **2019**. Ongoing hybridization obscures phylogenetic relationships in the *Drosophila subquinaria* species complex. *Journal of Evolutionary Biology* **32**: 1093–1105.

Gregory-Woodzicki KM. **2000**. Uploft history of the Central and Northern Andes: A Review. **112**: 1091–1105.

Hoorn C, Mosbrugger V, Mulch A, Antonelli A. **2013**. Biodiversity from mountain building. *Nature Geoscience* **6**: 154–154.

Hoorn C, Perrigo A, Antonelli A. **2018**. *Mountains, climate and biodiversity.* Hoboken: Wiley.

Hoorn C, Wesselingh FP, ter Steege H, Bermudez MA, Mora A, Sevink J, Sanmartin I, Sanchez-Meseguer A, Anderson CL, Figueiredo JP, *et al.* 2010. Amazonia Through Time: Andean Uplift, Climate Change, Landscape Evolution, and Biodiversity. *Science* **330**: 927–931.

Hughes C, Eastwood R. **2006**. Island radiation on a continental scale: Exceptional rates of plant diversification after uplift of the Andes. *Proceedings of the National Academy of Sciences* **103**: 10334–10339.

Jäger-Zürn I, Grubert M. **2000**. Podostemaceae Depend on Sticky Biofilms with Respect to Attachment to Rocks in Waterfalls. *International Journal of Plant Sciences* **161**: 599–607.

Janzen DH. **1967**. Why Mountain Passes are Higher in the Tropics. *The American Naturalist* **101**: 233–249.

Johnson MG, Gardner EM, Liu Y, Medina R, Goffinet B, Shaw AJ, Zerega NJC, Wickett NJ. **2016**. HybPiper: Extracting Coding Sequence and Introns for Phylogenetics from High-Throughput Sequencing Reads Using Target Enrichment. *Applications in Plant Sciences* **4**: 1600016.

Katayama N, Kato M, Imaichi R. **2016**. Habitat specificity enhances genetic differentiation in two species of aquatic Podostemaceae in Japan. *American Journal of Botany* **103**: 317–324.

669 **Kates HR, Johnson MG, Gardner EM, Zerega NJC, Wickett NJ**. **2018**. Allele phasing has
670 minimal impact on phylogenetic reconstruction from targeted nuclear gene sequences in a case
671 study of *Artocarpus*. *American Journal of Botany* **105**: 404–416.

672 **Katoh K, Standley DM**. **2013**. MAFFT Multiple Sequence Alignment Software Version 7:
673 Improvements in Performance and Usability. *Molecular Biology and Evolution* **30**: 772–780.

674 **Kattan G, Franco P, Rojas V, Morales G**. **2004**. A spatial analysis of faunistic diversity and
675 biogeography of the Andes of Colombia. **31**: 1829–1839.

676 **Kita Y, Kato M**. **2004**. Phylogenetic relationships between disjunctly occurring groups of
677 Tristicha trifaria (Podostemaceae): Phylogeny of Tristicha trifaria. *Journal of Biogeography* **31**:
678 1605–1612.

679 **Koi S, Ikeda H, Rutishauser R, Kato M**. **2015**. Historical biogeography of river-weeds
680 (Podostemaceae). *Aquatic Botany* **127**: 62–69.

681 **Lagomarsino LP, Condamine FL, Antonelli A, Mulch A, Davis CC**. **2016**. The abiotic and
682 biotic drivers of rapid diversification in Andean bellflowers (Campanulaceae). *New Phytologist*
683 **210**: 1430–1442.

684 **Latrubesse EM, Cozzuol M, da Silva-Caminha SAF, Rigsby CA, Absy ML, Jaramillo C**.
685 **2010**. The Late Miocene paleogeography of the Amazon Basin and the evolution of the Amazon
686 River system. *Earth-Science Reviews* **99**: 99–124.

687 **Leaché AD, Chavez AS, Jones LN, Grummer JA, Gottscho AD, Linkem CW**. **2015**.
688 Phylogenomics of Phrynosomatid Lizards: Conflicting Signals from Sequence Capture versus
689 Restriction Site Associated DNA Sequencing. *Genome Biology and Evolution* **7**: 706–719.

690 **Leaché AD, Harris RB, Rannala B, Yang Z**. **2014**. The Influence of Gene Flow on Species
691 Tree Estimation: A Simulation Study. *Systematic Biology* **63**: 17–30.

692 **Leleeka M, Sanavar D, Tandon R, Uniyal PL**. **2016**. Features of seeds of Podostemaceae and
693 their survival strategie in freshwater ecosystems. **26**: 29–36.

694 **Lujan NK, Armbruster JW**. **2011**. The Guiana Shield. In: Historical Biogeography of
695 Neotropical Freshwater Fishes. University of California Press, Berkeley., 211–224.

696 **Lujan NK, Armbruster JW, Werneke DC, Teixeira TF, Lovejoy NR**. **2019**. Phylogeny and
697 biogeography of the Brazilian–Guiana Shield endemic Corymbophanes clade of armoured
698 catfishes (Loricariidae). *Zoological Journal of the Linnean Society*: zlz090.

699 **Luna R, Guzmán-Merodio D, Núñez-Farfán J, Philbrick CT, Collazo-Ortega M, Márquez-**
700 **Guzmán J**. **2012**. Cross compatibility between Marathrum rubrum and Marathrum schiedeanum
701 (Podostemaceae), two closely related species of the Pacific Mexican Coast. *Aquatic Botany* **102**:
702 1–7.

Lundberg JG, Chernoff B. **1992**. A Miocene Fossil of the Amazonian Fish Arapaima (Teleostei, Arapaimidae) from the Magdalena River Region of Colombia--Biogeographic and Evolutionary Implications. *Biotropica* **24**: 2.

Madriñán S, Cortés AJ, Richardson JE. **2013**. Páramo is the world's fastest evolving and coolest biodiversity hotspot. *Frontiers in Genetics* **4**.

Magallón S, Gómez-Acevedo S, Sánchez-Reyes LL, Hernández-Hernández T. **2015**. A metacalibrated time-tree documents the early rise of flowering plant phylogenetic diversity. *New Phytologist* **207**: 437–453.

McCormack JE, Harvey MG, Faircloth BC, Crawford NG, Glenn TC, Brumfield RT. **2013**. A Phylogeny of Birds Based on Over 1,500 Loci Collected by Target Enrichment and High-Throughput Sequencing (N Alvarez, Ed.). *PLoS ONE* **8**: e54848.

McVay JD, Hipp AL, Manos PS. **2017**. A genetic legacy of introgression confounds phylogeny and biogeography in oaks. **284**.

Montes C, Rodriguez-Corcho AF, Bayona G, Hoyos N, Zapata S, Cardona A. **2019**. Continental margin response to multiple arc-continent collisions: The northern Andes-Caribbean margin. *Earth-Science Reviews* **198**: 102903.

Mora A, Baby P, Roddaz M, Parra M, Brusset S, Hermoza W, Espurt N. **2010**. Tectonic history of the Andes and sub-Andean zones: implications for the development of the Amazon drainage basin. In: Amazonia, Landscape and Species Evolution. Wiley, Oxford, 38–60.

Musilová Z, Kalous L, Petrtýl M, Chaloupková P. **2013**. Cichlid Fishes in the Angolan Headwaters Region: Molecular Evidence of the Ichthyofaunal Contact between the Cuanza and Okavango-Zambezi Systems (F Tinti, Ed.). *PLoS ONE* **8**: e65047.

Nevado B, Contreras-Ortiz N, Hughes C, Filatov DA. **2018**. Pleistocene glacial cycles drive isolation, gene flow and speciation in the high-elevation Andes. *New Phytologist* **219**: 779–793.

Novelo RA, Philbrick CT. **1997**. Taxonomy of Mexican Podostemaceae. *Aquatic Botany* **57**: 275–303.

Novelo RA, Philbrick CT, Crow GE. **2009**. Podostemaceae. In: Flora Mesoamericana. 1–7.

Nürk NM, Scheriau C, Madriñán S. **2013**. Explosive radiation in high Andean Hypericum—rates of diversification among New World lineages. *Frontiers in Genetics* **4**.

One Thousand Plant Transcriptomes Initiative. **2019**. One thousand plant transcriptomes and the phylogenomics of green plants. *Nature* **574**: 679–685.

Parra M, Echeverri S, Patiño AM, Ramírez JC, Mora A, Sobel ER, Almendral A, Pardo-Trujillo A. **2019**. Cenozoic evolution of the Sierra Nevada de Santa Marta, Colombia. In: The geology of Colombia, Volume 3 Paleogene-Neogene. Bogotá: Servicio Geológico Colombiano, Publicaciones Geológicas Especiales, 259–297.

Pérez-Escobar OA, Chomicki G, Condamine FL, Karremans AP, Bogarín D, Matzke NJ, Silvestro D, Antonelli A. **2017**. Recent origin and rapid speciation of Neotropical orchids in the world's richest plant biodiversity hotspot. *New Phytologist* **215**: 891–905.

Peterson BK, Weber JN, Kay EH, Fisher HS, Hoekstra HE. **2012**. Double Digest RADseq: An Inexpensive Method for De Novo SNP Discovery and Genotyping in Model and Non-Model Species (L Orlando, Ed.). *PLoS ONE* **7**: e37135.

Philbrick CT, Bove CP, Stevens HI. **2010**. Endemism in Neotropical Podostemaceae [1]. *Annals of the Missouri Botanical Garden* **97**: 425–456.

Philbrick CT, Novelo RA. **1995**. New World Podostemaceae: Ecological and Evolutionary Enigmas. *Brittonia* **47**: 210.

Philbrick CT, Novelo A. **1997**. Ovule number, seed number and seed size in Mexican and North American species of Podostemaceae. *Aquatic Botany* **57**: 183–200.

Philbrick CT, Novelo RA. **1998**. Flowering phenology, pollen flow, and seed production in Marathrum rubrum (Podostemaceae). *Aquatic Botany* **62**: 199–206.

Picq S, Alda F, Krahe R, Bermingham E. **2014**. Miocene and Pliocene colonization of the Central American Isthmus by the weakly electric fish *Brachyhypopomus occidentalis* (Hypopomidae, Gymnotiformes) (M Ebach, Ed.). *Journal of Biogeography* **41**: 1520–1532.

Puritz JB, Hollenbeck CM, Gold JR. **2014**. dDocent: a RADseq, variant-calling pipeline designed for population genomics of non-model organisms. *PeerJ* **2**: e431.

Quintero I, Jetz W. **2018**. Global elevational diversity and diversification of birds. *Nature* **555**: 246–250.

Rambaut A, Drummond AJ, Xie D, Baele G, Suchard MA. **2018**. Posterior Summarization in Bayesian Phylogenetics Using Tracer 1.7 (E Susko, Ed.). *Systematic Biology* **67**: 901–904.

Reyes-Ortega I, Sánchez-Coronado ME, Orozco-Segovia A. **2009**. Seed germination in Marathrum schiedeanum and M. rubrum (Podostemaceae). *Aquatic Botany* **90**: 13–17.

Richardson JE, Madriñán S, Gómez-Gutiérrez MC, Valderrama E, Luna J, Banda-R. K, Serrano J, Torres MF, Jara OA, Aldana AM, *et al.* 2018. Using dated molecular phylogenies to help reconstruct geological, climatic, and biological history: Examples from Colombia (I Somerville, Ed.). *Geological Journal* **53**: 2935–2943.

Rodríguez-Muñoz E, Montes C, Crawford AJ. **2020**. *Synthesis of geological and comparative phylogeographic data point to climate, not mountain uplift, as driver of divergence across the Eastern Andean Cordillera*. Evolutionary Biology.

Ronquist F, Huelsenbeck JP. **2003**. MrBayes 3: Bayesian phylogenetic inference under mixed models. *Bioinformatics* **19**: 1572–1574.

Roxo FF, Albert JS, Silva GSC, Zawadzki CH, Foresti F, Oliveira C. **2014**. Molecular Phylogeny and Biogeographic History of the Armored Neotropical Catfish Subfamilies Hypoptopomatinae, Neoplecostominae and Otothyrinae (Siluriformes: Loricariidae) (HT Lumbsch, Ed.). *PLoS ONE* **9**: e105564.

van Royen P. **1951**. *The Podostemaceae of the New World*. Harte.

Ruhfel BR, Bove CP, Philbrick CT, Davis CC. **2016**. Dispersal largely explains the Gondwanan distribution of the ancient tropical clusioid plant clade. *American Journal of Botany* **103**: 1117–1128.

Ruokolainen K, Moulatlet GM, Zuquim G, Hoorn C, Tuomisto H. **2019**. Geologically recent rearrangements in central Amazonia river network and their importance for the riverine barrier hypothesis. **11**: e45046.

Rutishauser R. **1995**. Developmental patterns of leaves in Podostemaceae compared with more typical flowering plants: saltational evolution and fuzzy morphology. *Canadian Journal of Botany* **73**: 1305–1317.

Rutishauser R. **1997**. Structural and developmental diversity in Podostemaceae (river-weeds). *Aquatic Botany* **57**: 29–70.

Rutishauser R, Novelo RA, Philbrick CT. **1999**. Developmental Morphology of New World Podostemaceae: Marathrum and Vanroyenella. *International Journal of Plant Sciences* **160**: 29–45.

Schmickl R, Liston A, Zeisek V, Oberlander K, Weitemier K, Straub SCK, Cronn RC, Dreyer LL, Suda J. **2016**. Phylogenetic marker development for target enrichment from transcriptome and genome skim data: the pipeline and its application in southern African *Oxalis* (Oxalidaceae). *Molecular Ecology Resources* **16**: 1124–1135.

Sklenář P, Dušková E, Balslev H. **2011**. Tropical and Temperate: Evolutionary History of Páramo Flora. *The Botanical Review* **77**: 71–108.

Smith BT, McCormack JE, Cuervo AM, Hickerson MichaelJ, Aleixo A, Cadena CD, Pérez-Emán J, Burney CW, Xie X, Harvey MG, *et al.* 2014. The drivers of tropical speciation. *Nature* **515**: 406–409.

Stamatakis A. **2014**. RAxML version 8: a tool for phylogenetic analysis and post-analysis of large phylogenies. *Bioinformatics* **30**: 1312–1313.

Stenz NWM, Larget B, Baum DA, Ané C. **2015**. Exploring Tree-Like and Non-Tree-Like Patterns Using Genome Sequences: An Example Using the Inbreeding Plant Species *Arabidopsis thaliana* (L.) Heynh. *Systematic Biology* **64**: 809–823.

Tagliacollo VA, Roxo FF, Duke-Sylvester SM, Oliveira C, Albert JS. **2015**. Biogeographical signature of river capture events in Amazonian lowlands. *Journal of Biogeography* **42**: 2349–2362.

Testo WL, Sessa E, Barrington DS. **2019**. The rise of the Andes promoted rapid diversification in Neotropical *Phlegmariurus* (Lycopodiaceae). *New Phytologist* **222**: 604–613.

Than C, Ruths D, Nakhleh L. **2008**. PhyloNet: a software package for analyzing and reconstructing reticulate evolutionary relationships. *BMC Bioinformatics* **9**: 322.

Tippery NP, Philbrick CT, Bove CP, Les DH. **2011**. Systematics and Phylogeny of Neotropical Riverweeds (Podostemaceae: Podostemoideae). *Systematic Botany* **36**: 105–118.

Villagómez D, Spikings R, Mora A, Guzmán G, Ojeda G, Cortés E, van der Lelij R. **2011**. Vertical tectonics at a continental crust-oceanic plateau plate boundary zone: Fission track thermochronology of the Sierra Nevada de Santa Marta, Colombia: THERMOCHRONOLOGY OF NORTHERN COLOMBIA. *Tectonics* **30**: n/a-n/a.

Wagner CE, Keller I, Wittwer S, Selz OM, Mwaiko S, Greuter L, Sivasundar A, Seehausen O. **2013**. Genome-wide RAD sequence data provide unprecedented resolution of species boundaries and relationships in the Lake Victoria cichlid adaptive radiation. *Molecular Ecology* **22**: 787–798.

Wascher M, Kubatko L. **2020**. Consistency of SVDQuartets and Maximum Likelihood for Coalescent-Based Species Tree Estimation (E Susko, Ed.). *Systematic Biology*: syaa039.

Wen D, Yu Y, Zhu J, Nakhleh L. **2018**. Inferring Phylogenetic Networks Using PhyloNet (D Posada, Ed.). *Systematic Biology* **67**: 735–740.

Willis JC. **1902**. Studies in the morphology and ecology of the Podostemaceae of Ceylon and India. **1**: 267–465.

Willis JC. **1914**. On the lack of adaptation in the Tristichaceae and Podostemaceae. **87**: 532–550.

Willis JC. **1915**. The origin of the Tristichaceae and Podostemaceae. **29**: 299–306.

Yuan Y-W, Liu C, Marx HE, Olmstead RG. **2009**. The pentatricopeptide repeat (PPR) gene family, a tremendous resource for plant phylogenetic studies: Methods. *New Phytologist* **182**: 272–283.

Yuan Y-W, Liu C, Marx HE, Olmstead RG. **2010**. An empirical demonstration of using pentatricopeptide repeat (PPR) genes as plant phylogenetic tools: Phylogeny of Verbenaceae and the Verbena complex. *Molecular Phylogenetics and Evolution* **54**: 23–35.

Zhang L-N, Ma P-F, Zhang Y-X, Zeng C-X, Zhao L, Li D-Z. **2019**. Using nuclear loci and allelic variation to disentangle the phylogeny of Phyllostachys (Poaceae, Bambusoideae). *Molecular Phylogenetics and Evolution* **137**: 222–235.

Zhang C, Rabiee M, Sayyari E, Mirarab S. **2018**. ASTRAL-III: polynomial time species tree reconstruction from partially resolved gene trees. *BMC Bioinformatics* **19**: 153.

842 **Zimmermann T, Mirarab S, Warnow T**. **2014**. BBCA: Improving the scalability of *BEAST
843 using random binning. *BMC Genomics* **15**: S11.

844

Table 1. Results of our calibration and the calibrations for the same node inferred in two previous studies. Ruhfel et al., presented two dating results for alternative placements of the fossil *Paleoclusia chevalieri*

	Bedoya et al., 2020	Magallón et al., 2015	Ruhfel et al., 2016	
95% HPD Min (Ma)	54.56	53.53	49.9	55.4
95% HPD Mean (Mya)	62.43	67.82	62	66.1
95% HPD Max (Mya)	70.30	77.29	71.9	76.8

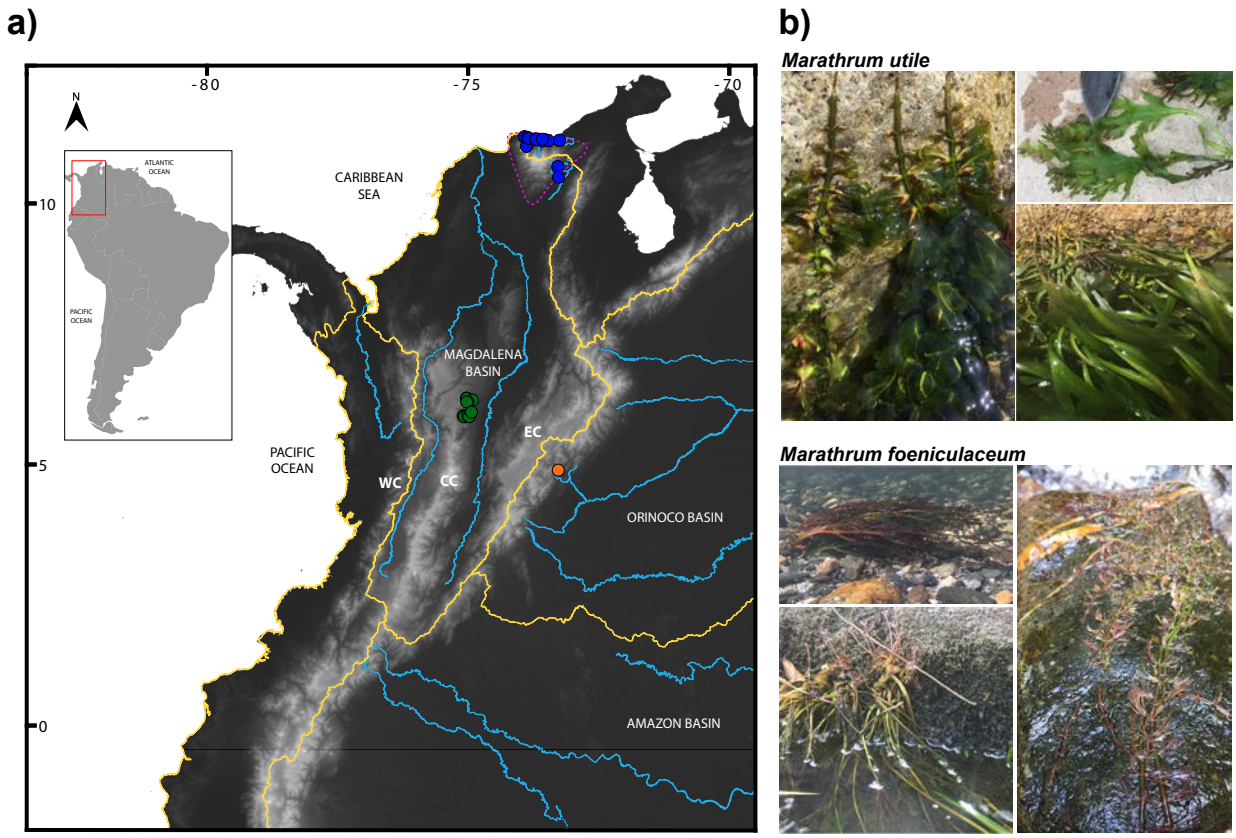

Figure 1. a) Localities where *Marathrum* specimens were sampled (dots). Green=Antioquia, Blue=Caribe, Orange=Boyacá. The three Andean Cordilleras are shown. WC= Western Cordillera, CC=Central cordillera, EC=Eastern Cordillera. Yellow lines delimit drainage basins. The Sierra Nevada de Santa Marta is indicated with pink dashed lines. Major rivers are shown in blue. b) Phenotype of *M. utile* and *M. foeniculaceum*. The former one has laminar, entire leaves. The latter has highly dissected leaves. Flower morphology varies geographically in both species.

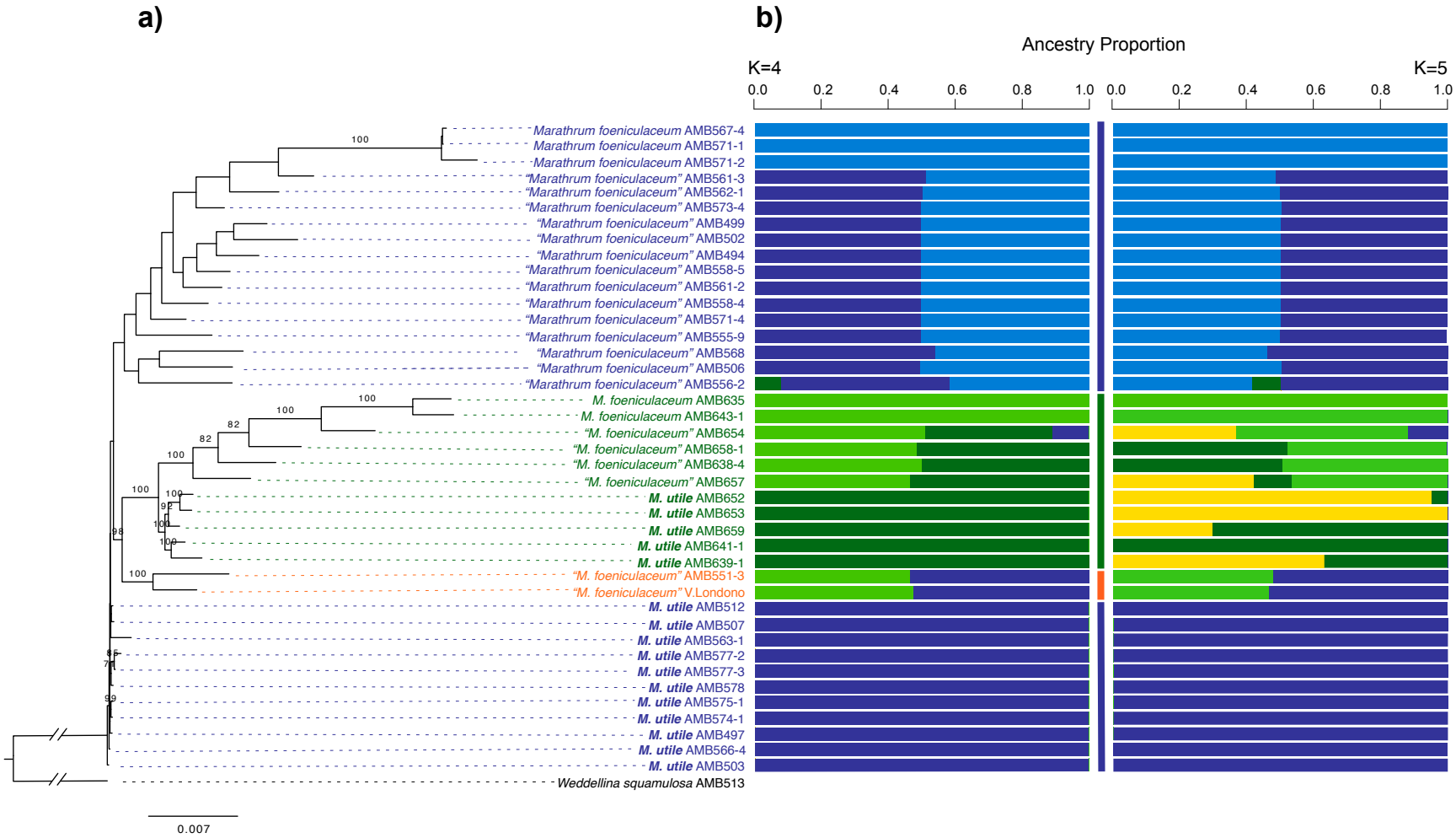

Figure 2. Phylogenetic relationships and ancestry proportion of individuals from Antioquia (green), Caribe (blue) and Boyacá (orange) inferred from target enrichment data. a) Maximum likelihood tree inferred from concatenated analyses of 207 targeted loci. Bootstrap support (≥70) is shown above branches. Admixed individuals are indicated with quotation marks. b) Ancestry proportions for K=4 and K=5 inferred with ADMIXTURE. Vertical bars indicate the drainage basin where each individual was collected.

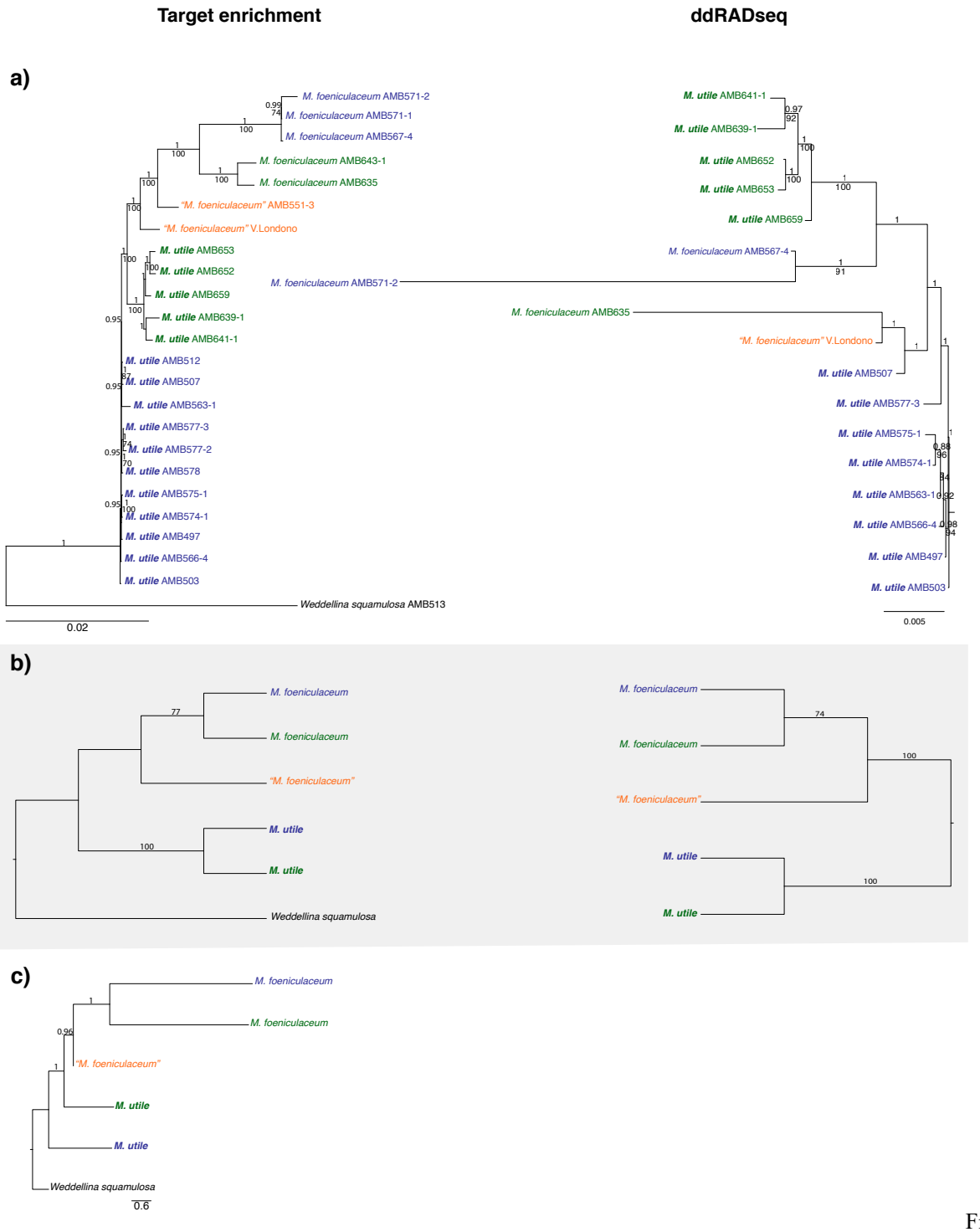

Figure 3. Phylogenetic trees inferred using data concatenation and species tree inference on target enrichment and ddRADseq data excluding admixed individuals from Antioquia and Caribe. The provenance of individuals is indicated in green (Antioquia), blue (Caribe), and orange (Boyacá). ddRADseq topologies are rooted based on results from target enrichment. Admixed individuals as inferred with ADMIXTURE are indicated with quotation marks. a) Majority rule consensus bayesian trees inferred from concatenated data. Posterior probabilities ≥0.7 are shown above branches. Bootstrap support (≥70) from ML reconstruction are shown below branches. b) Species tree inferred with SVDquartets. Quarter support values >70 shown above branches. c) Species tree inferred with ASTRAL III for the target enrichment dataset. Local posterior probabilities > 0.7 shown above branches.

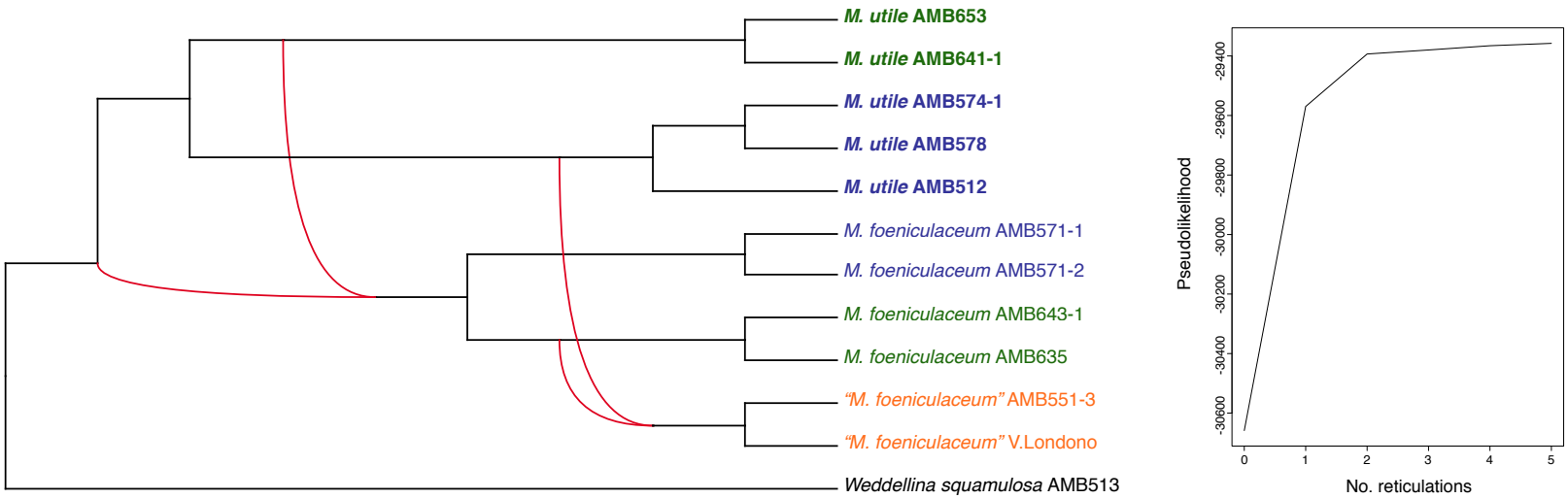

Figure 4. Phylogenetic network resulted from maximum pseudo-likelihood inference with PhyloNet. After 2 reticulation events, the pseudolikelihood score starts to plateau. Provenance of samples is shown in green (Antioquia), blue (Caribe), and orange (Boyacá). Admixed individuals as inferred with ADMIXTURE are indicated with quotation marks. Inferred reticulation events are depicted with red lines.

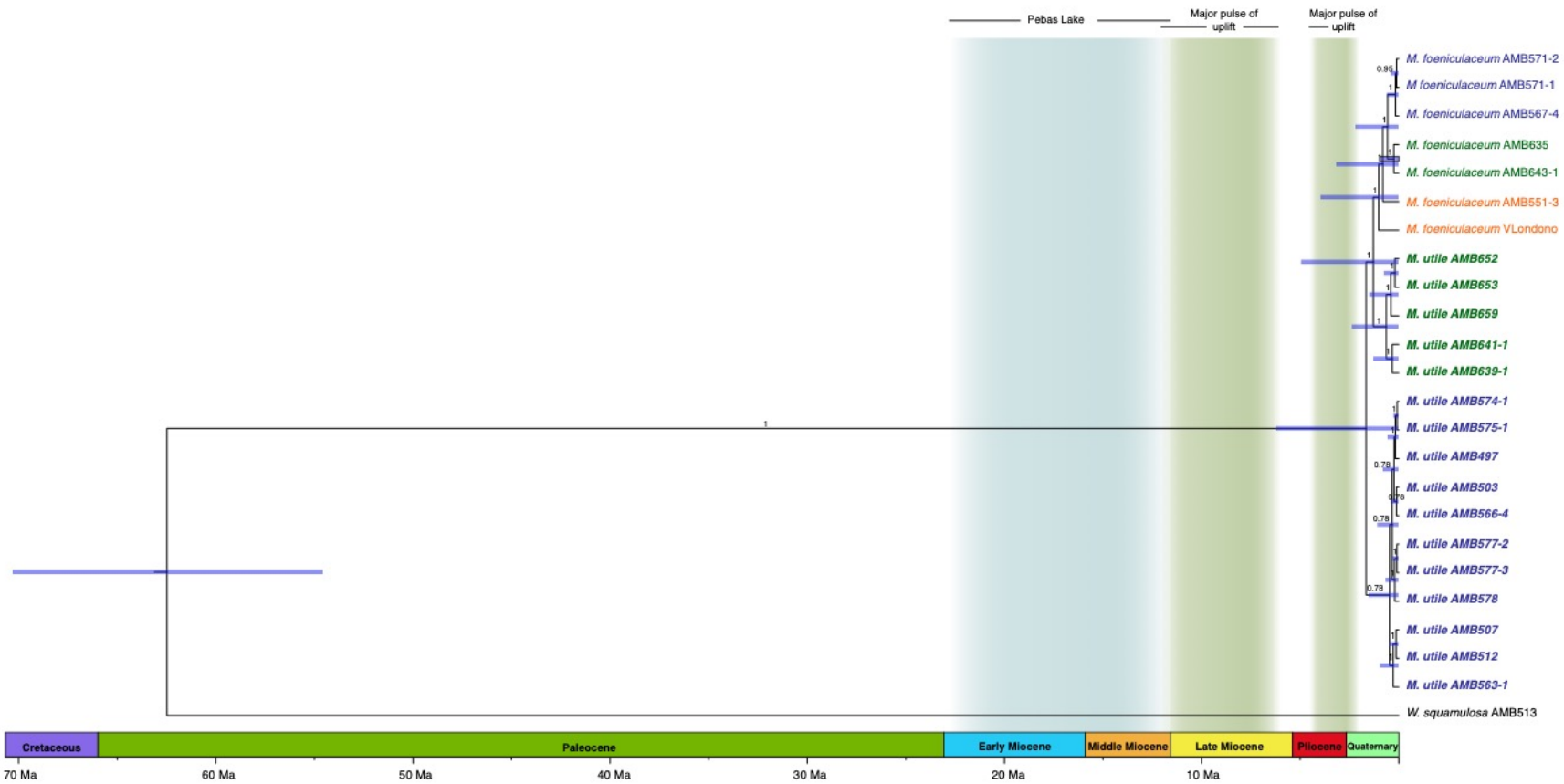

Figure 5. Divergence time tree inferred from *BEAST. Vertical bars indicate hypothesized landscape features and geological events. Blue horizontal bars indicate the 95% HPD. Posterior probabilities are shown above branches. The provenance of individuals is indicated in green (Antioquia), blue (Caribe), and orange (Boyacá).

Supplementary Materials

Table S1. Voucher numbers, NCBI accessions and locations for the samples collected and included in this study. Samples are arranged by species. Admixed individuals are indicated in quotations marks, and individuals that have the phenotype of *M. foeniculaceum* but whose genetic constitution was not assessed with admixture are indicated as morphs since they could correspond to *M. foeniculaceum* or to hybrids. The sample used for generating genome-skimming data is in bold (SRR12956182 for WGS read data). Genomic data are deposited in the NCBI Sequence Read Archive under Bioproject PRJNA673497.

Collector No	SRA accession # ddRADseq	SRA accession # target enrichment	GenBank accession numbers	Species	Coordinates	Basin/River
AMB 497	**SRR12971533**	**SRR12975804**	**-**	***Marathrum utile***	**11°11'47.07"N, 73°27'35.53"W**	**Caribe/Ancho**
AMB 503	SRR12989095	SRR12983242	-	*Marathrum utile*	11°11'33.46"N, 73°34'59.01"W	Caribe/Chorro Catalina
AMB 507	SRR12971532	SRR12975803	-	*Marathrum utile*	11°6'13.93"N, 73°52'19.28"W	Caribe/Buritaca
AMB 508	SRR12971530	-	-	*Marathrum utile*	11°6'13.93"N, 73°52'19.28"W	Caribe/Buritaca
AMB 509	SRR12971529	-	-	*Marathrum utile*	11°6'13.93"N, 73°52'19.28"W	Caribe/Buritaca
AMB 512	FAILED	SRR12975802	-	*Marathrum utile*	11°5'34.16"N, 73°53'12.51"W	Caribe/Buritaca
AMB 563-1	SRR12971527	SRR12975801	-	*Marathrum utile*	11°13'30"N, 73°41'50"W	Caribe/Don Diego
AMB 563-3	SRR12971526	-	-	*Marathrum utile*	11°13'30"N, 73°41'50"W	Caribe/Don Diego
AMB 563-4	SRR12971525	-	-	*Marathrum utile*	11°13'30"N, 73°41'50"W	Caribe/Don Diego
AMB 566-1	SRR12971524	-	-	*Marathrum utile*	11°12'2"N, 73°27'42"W	Caribe/Ancho
AMB 566-3	SRR12971523	-	-	*Marathrum utile*	11°12'2"N, 73°27'42"W	Caribe/Ancho
AMB 566-4	SRR12971522	SRR12975800	-	*Marathrum utile*	11°12'2"N, 73°27'42"W	Caribe/Ancho
AMB 566-6	SRR12971521	-	-	*Marathrum utile*	11°12'2"N, 73°27'42"W	Caribe/Ancho
AMB 566-8	SRR12971519	-	-	*Marathrum utile*	11°12'2"N, 73°27'42"W	Caribe/Ancho
AMB 566-9	SRR12971518	-	-	*Marathrum utile*	11°12'2"N, 73°27'42"W	Caribe/Ancho
AMB 566-14	SRR12971517	-	-	*Marathrum utile*	11°12'2"N, 73°27'42"W	Caribe/Ancho
AMB 566-18	SRR12971516	-	-	*Marathrum utile*	11°12'2"N, 73°27'42"W	Caribe/Ancho
AMB 574-1	SRR12971515	SRR12975799	-	*Marathrum utile*	11°12'39"N, 73°15'8"W	Caribe/Jerez
AMB 574-2	SRR12971514	-	-	*Marathrum utile*	11°12'39"N, 73°15'8"W	Caribe/Jerez
AMB 575-1	SRR12971513	SRR12975798	-	*Marathrum utile*	11°12'39"N, 73°15'8"W	Caribe/Jerez
AMB 575-2	SRR12971512	-	-	*Marathrum utile*	11°12'39"N, 73°15'8"W	Caribe/Jerez
AMB 575-3	SRR12971511	-	-	*Marathrum utile*	11°12'39"N, 73°15'8"W	Caribe/Jerez
AMB 577-1	SRR12971510	-	-	*Marathrum utile*	10°42'25"N, 73°17'4"W	Caribe/Jerez
AMB 577-2	FAILED	SRR12975797	-	*Marathrum utile*	10°42'25"N, 73°17'4"W	Caribe/Badillo
AMB 577-3	SRR12971507	SRR12975796	-	*Marathrum utile*	10°42'25"N, 73°17'4"W	Caribe/Badillo
AMB 578	-	SRR12983243	-	*Marathrum utile*	10°30'5"N, 73°16'9"W	Caribe/Guatapurí
AMB 639-1	SRR12971506	SRR12975795	-	*Marathrum utile*	6°16'0"N, 75°1'45"W	Antioquia/Arenal
AMB 639-2	SRR12971505	-	-	*Marathrum utile*	6°16'0"N, 75°1'45"W	Antioquia/Arenal
AMB 639-3	SRR12971504	-	-	*Marathrum utile*	6°16'0"N, 75°1'45"W	Antioquia/Arenal
AMB 639-4	SRR12971503	-	-	*Marathrum utile*	6°16'0"N, 75°1'45"W	Antioquia/Arenal
AMB 639-5	SRR12971502	-	-	*Marathrum utile*	6°16'0"N, 75°1'45"W	Antioquia/Arenal
AMB 641-1	SRR12971501	SRR12975793	-	*Marathrum utile*	6°13'57"N, 74°54'58"W	Antioquia/Arenal
AMB 641-2	SRR12971500	-	-	*Marathrum utile*	6°13'57"N, 74°54'58"W	Antioquia/Arenal
AMB 641-3	SRR12971499	-	-	*Marathrum utile*	6°13'57"N, 74°54'58"W	Antioquia/Arenal
AMB 642-1	FAILED	FAILED	-	*Marathrum utile*	6°13'57"N, 74°54'58"W	Antioquia/Arenal
AMB 642-2	SRR12971497	-	-	*Marathrum utile*	6°13'57"N, 74°54'58"W	Antioquia/Arenal
AMB 651	SRR12971596	-	-	*Marathrum utile*	5°55'58"N, 75°5'45"W	Antioquia/Santo Domingo
AMB 652	SRR12971595	SRR12975792	-	*Marathrum utile*	5°55'58"N, 75°5'45"W	Antioquia/Santo Domingo
AMB 653	SRR12971594	SRR12975791	-	*Marathrum utile*	5°54'51"N, 75°4'28"W	Antioquia/Santo Domingo

AMB 659	SRR12971593	SRR12975790	-	*Marathrum utile*	6°0'2"N, 74°56'15"W	Antioquia/Samaná Norte
AMB 567-4	SRR12971578	SRR12975808	-	*Marathrum foeniculaceum*	11°12'2"N, 73°27'42"W	Caribe/Ancho
AMB 571-1	FAILED	SRR12975807	-	*Marathrum foeniculaceum*	11°13'46"N, 73°34'40"W	Caribe/Palomino
AMB 571-2	SRR12971576	SRR12975806	-	*Marathrum foeniculaceum*	11°13'46"N, 73°34'40"W	Caribe/Palomino
AMB 635	SRR13013619	SRR12983247	-	*Marathrum foeniculaceum*	6°16'4"N, 75°1'49"W	Antioquia/Arenal
AMB 643-1	-	SRR12983246		*Marathrum foeniculaceum*	6°13'57"N, 74°54'58"W	Antioquia/Arenal
AMB 494	SRR12971587	SRR12975817	-	*"Marathrum foeniculaceum"*	11°13'7.63"N, 73°42'0.14"W	Caribe/Don Diego
AMB 499	SRR12971586	SRR12975816	-	*"Marathrum foeniculaceum"*	11°12'22.95"N, 73°15'17.26"W	Caribe/Jerez
AMB 502	SRR12971575	SRR12975805	-	*"Marathrum foeniculaceum"*	11°11'33.46"N, 73°34'59.01"W	Caribe/Chorro Catalina
AMB 506	SRR13013618	SRR12983248	-	*"Marathrum foeniculaceum"*	11°16'33.96"N, 73°55'26.57"W	Caribe/ Piedras
AMB 551-3	-	SRR12983244		*"Marathrum foeniculaceum"*	4°53'29"N, 73°16'31"W	Boyacá/Batá
AMB 555-9	SRR12971564	SRR12975794	-	*"Marathrum foeniculaceum"*	11°16'33.96"N, 73°55'26.57"W	Caribe/Piedras
AMB 556-2	SRR12971553	SRR12975789	-	*"Marathrum foeniculaceum"*	11°16'0"N, 73°51'56"W	Caribe/Mendihuaca
AMB 558-4	SRR12971542	SRR12975788	-	*"Marathrum foeniculaceum"*	11°14'41"N, 73°50'35"W	Caribe/Guachaca
AMB 558-5	SRR12971531	SRR12975787	-	*"Marathrum foeniculaceum"*	11°14'41"N, 73°50'35"W	Caribe/Guachaca
AMB 561-2	SRR12971520	SRR12975786	-	*"Marathrum foeniculaceum"*	11°14'11"N, 73°41'51"W	Caribe/Don Diego
AMB 561-3	SRR12971509	SRR12975785	-	*"Marathrum foeniculaceum"*	11°14'11"N, 73°41'51"W	Caribe/Don Diego
AMB 562-1	SRR12971498	SRR12975784	-	*"Marathrum foeniculaceum"*	11°13'56"N, 73°42'2"W	Caribe/Don Diego
AMB 568	SRR12971585	SRR12975815	-	*"Marathrum foeniculaceum"*	11°12'2"N, 73°27'42"W	Caribe/Ancho
AMB 571-4	SRR12971584	SRR12975814	-	*"Marathrum foeniculaceum"*	11°13'46"N, 73°34'40"W	Caribe/Palomino
AMB 573-4	FAILED	SRR12975813	-	*"Marathrum foeniculaceum"*	11°12'39"N, 73°15'8"W	Caribe/Jerez
AMB 638-4	SRR12971582	SRR12975812	-	*"Marathrum foeniculaceum"*	6°16'0"N, 75°1'45"W	Antioquia/Arenal
AMB 654	SRR12971581	SRR12975811	-	*"Marathrum foeniculaceum"*	5°54'51"N, 75°4'28"W	Antioquia/Santo Domingo
AMB 657	SRR13013620	SRR12983245	-	*"Marathrum foeniculaceum"*	5°54'56"N, 74°58'45"W	Antioquia/Samaná Norte
AMB 658-1	SRR12971580	SRR12975810	-	*"Marathrum foeniculaceum"*	6°0'2"N, 74°56'15"W	Antioquia/Samaná Norte
V.Londono	SRR12971579	SRR12975809	-	*"Marathrum foeniculaceum"*	4°53'29"N, 73°16'31"W	Boyacá/Batá
AMB 492	FAILED	-	-	*Marathrum foeniculaceum* (morph)	11°13'7.63"N, 73°42'0.14"W	Caribe/Don Diego
AMB 493	SRR12971574	-	-	*Marathrum foeniculaceum* (morph)	11°13'7.63"N, 73°42'0.14"W	Caribe/Don Diego
AMB 495	FAILED	-	-	*Marathrum foeniculaceum* (morph)	11°13'19.31"N, 73°31'38.01"W	Caribe/San Salvador
AMB 496	SRR12971573	-	-	*Marathrum foeniculaceum* (morph)	11°13'19.31"N, 73°31'38.01"W	Caribe/San Salvador
AMB 498	FAILED	-	-	*Marathrum foeniculaceum* (morph)	11°11'47.07"N, 73°27'35.53"W	Caribe/Ancho
AMB 500	SRR12971572	-	-	*Marathrum foeniculaceum* (morph)	11°12'22.95"N, 73°15'17.26"W	Caribe/Jerez
AMB 551-4	SRR12971571	-	-	*Marathrum foeniculaceum* (morph)	4°53'29"N, 73°16'31"W	Boyacá/Batá
AMB 551-5	SRR12971570	-	-	*Marathrum foeniculaceum* (morph)	4°53'29"N, 73°16'31"W	Boyacá/Batá
AMB 551-6	SRR12971569	-	-	*Marathrum foeniculaceum* (morph)	4°53'29"N, 73°16'31"W	Boyacá/Batá
AMB 551-7	SRR12971568	-	-	*Marathrum foeniculaceum* (morph)	4°53'29"N, 73°16'31"W	Boyacá/Batá
AMB 551-8	SRR12971567	-	-	*Marathrum foeniculaceum* (morph)	4°53'29"N, 73°16'31"W	Boyacá/Batá
AMB 551-10	SRR12971566	-	-	*Marathrum foeniculaceum* (morph)	4°53'29"N, 73°16'31"W	Boyacá/Batá
AMB 556-1	SRR12971565	-	-	*Marathrum foeniculaceum* (morph)	11°16'0"N, 73°51'56"W	Caribe/Mendihuaca
AMB 556-3	SRR12971563	-	-	*Marathrum foeniculaceum* (morph)	11°16'0"N, 73°51'56"W	Caribe/Mendihuaca
AMB 556-4	SRR12971562	-	-	*Marathrum foeniculaceum* (morph)	11°16'0"N, 73°51'56"W	Caribe/Mendihuaca
AMB 556-5	SRR12971561	-	-	*Marathrum foeniculaceum* (morph)	11°16'0"N, 73°51'56"W	Caribe/Mendihuaca
AMB 558-1	SRR12971560	-	-	*Marathrum foeniculaceum* (morph)	11°14'41"N, 73°50'35"W	Caribe/Guachaca
AMB 558-2	SRR12971559	-	-	*Marathrum foeniculaceum* (morph)	11°14'41"N, 73°50'35"W	Caribe/Guachaca
AMB 558-8	SRR12971558	-	-	*Marathrum foeniculaceum* (morph)	11°14'41"N, 73°50'35"W	Caribe/Guachaca
AMB 558-10	SRR12971557	-	-	*Marathrum foeniculaceum* (morph)	11°14'41"N, 73°50'35"W	Caribe/Guachaca
AMB 558-11	SRR12971556	-	-	*Marathrum foeniculaceum* (morph)	11°14'41"N, 73°50'35"W	Caribe/Guachaca
AMB 562-2	SRR12971555	-	-	*Marathrum foeniculaceum* (morph)	11°13'56"N, 73°42'2"W	Caribe/Don Diego
AMB 562-5	SRR12971554	-	-	*Marathrum foeniculaceum* (morph)	11°13'56"N, 73°42'2"W	Caribe/Don Diego
AMB 567-3	SRR12971552	-	-	*Marathrum foeniculaceum* (morph)	11°12'2"N, 73°27'42"W	Caribe/Ancho

AMB 567-5	FAILED	-	-	*Marathrum foeniculaceum* (morph)	11°12'2"N, 73°27'42"W	Caribe/Ancho
AMB 567-6	SRR12971551	-	-	*Marathrum foeniculaceum* (morph)	11°12'2"N, 73°27'42"W	Caribe/Ancho
AMB 567-7	SRR12971550	-	-	*Marathrum foeniculaceum* (morph)	11°12'2"N, 73°27'42"W	Caribe/Ancho
AMB 571-3	FAILED	-	-	*Marathrum foeniculaceum* (morph)	11°13'46"N, 73°34'40"W	Caribe/Palomino
AMB 571-5	SRR12971549	-	-	*Marathrum foeniculaceum* (morph)	11°13'46"N, 73°34'40"W	Caribe/Palomino
AMB 571-6	SRR12971548	-	-	*Marathrum foeniculaceum* (morph)	11°13'46"N, 73°34'40"W	Caribe/Palomino
AMB 573-1	SRR12971547	-	-	*Marathrum foeniculaceum* (morph)	11°12'39"N, 73°15'8"W	Caribe/Jerez
AMB 573-2	SRR12971546	-	-	*Marathrum foeniculaceum* (morph)	11°12'39"N, 73°15'8"W	Caribe/Jerez
AMB 573-3	SRR12971545	-	-	*Marathrum foeniculaceum* (morph)	11°12'39"N, 73°15'8"W	Caribe/Jerez
AMB 573-5	SRR12971544	-	-	*Marathrum foeniculaceum* (morph)	11°12'39"N, 73°15'8"W	Caribe/Jerez
AMB 573-6	SRR12971543	-	-	*Marathrum foeniculaceum* (morph)	11°12'39"N, 73°15'8"W	Caribe/Jerez
AMB 631-2	SRR12971541	-	-	*Marathrum foeniculaceum* (morph)	6°16'11"N, 75°1'54"W	Antioquia/Arenal
AMB 631-4	FAILED	-	-	*Marathrum foeniculaceum* (morph)	6°16'11"N, 75°1'54"W	Antioquia/Arenal
AMB 632	FAILED	FAILED	-	*Marathrum foeniculaceum* (morph)	6°16'11"N, 75°1'54"W	Antioquia/Arenal
AMB 636	SRR12971540	-	-	*Marathrum foeniculaceum* (morph)	6°16'0"N, 75°1'45"W	Antioquia/Arenal
AMB 638-3	SRR12971539	-	-	*Marathrum foeniculaceum* (morph)	6°16'0"N, 75°1'45"W	Antioquia/Arenal
AMB 640	SRR12971538	-	-	*Marathrum foeniculaceum* (morph)	6°16'0"N, 75°1'45"W	Antioquia/Arenal
AMB 642-3	FAILED	-	-	*Marathrum foeniculaceum* (morph)	6°13'57"N, 74°54'58"W	Antioquia/Arenal
AMB 645-1	SRR12971537	FAILED	-	*Marathrum foeniculaceum* (morph)	6°11'38"N, 75°0'18"W	Antioquia/Bañadero San Carlos
AMB 646-1	FAILED	FAILED	-	*Marathrum foeniculaceum* (morph)	6°11'52"N, 75°1'41"W	Antioquia/
AMB 646-4	SRR12971536	-	-	*Marathrum foeniculaceum* (morph)	6°11'52"N, 75°1'41"W	Antioquia/
AMB 646-5	FAILED	-	-	*Marathrum foeniculaceum* (morph)	6°11'52"N, 75°1'41"W	Antioquia/
AMB 646-6	FAILED	-	-	*Marathrum foeniculaceum* (morph)	6°11'52"N, 75°1'41"W	Antioquia/
AMB 655	SRR12971535	-	-	*Marathrum foeniculaceum* (morph)	5°55'44"N, 75°0'44"W	Antioquia/Samaná Norte
AMB 656-1	SRR12971534	-	-	*Marathrum foeniculaceum* (morph)	5°54'56"N, 74°58'45"W	Antioquia/Samaná Norte
AMB 658-2	FAILED	-	-	*Marathrum foeniculaceum* (morph)	6°0'2"N, 74°56'15"W	Antioquia/Samaná Norte
AMB 513	FAILED	SRR1298324	-	*Weddellina squamulosa*	0°51'42.9"N, 71°0'47.5"W	Amazonas/Vaupés
AMB 514	FAILED	-	-	*Weddellina squamulosa*	0°51'42.9"N, 71°0'47.5"W	Amazonas/Vaupés
AMB 515	FAILED	-	-	*Weddellina squamulosa*	0°51'42.9"N, 71°0'47.5"W	Amazonas/Vaupés
-	-	-	NC_036341	*Garcinia mangostana*	-	-
BNDE	-	-		*Hypericum perforatum*	-	-
-	-	-	KT337313.1	*Populus tremula*	-	-

Table S2. Number of loci for which N taxa have data. Ipyrad results for the assembly of all 96 ddRADseq samples and for minimum 4 individuals per loci.

N	Locus coverage	Sum coverage	N	Locus coverage	Sum coverage	N	Locus coverage	Sum coverage
1	0	0	**38**	154	168201	**75**	0	169462
2	0	0	**39**	136	168337	**76**	1	169463
3	0	0	**40**	123	168460	**77**	2	169465
4	46519	46519	**41**	105	168565	**78**	1	169466
5	28200	74719	**42**	86	168651	**79**	4	169470
6	20962	95681	**43**	73	168724	**80**	2	169472
7	13485	109166	**44**	75	168799	**81**	1	169473
8	10892	120058	**45**	89	168888	**82**	0	169473
9	7606	127664	**46**	68	168956	**83**	1	169474
10	6563	134227	**47**	75	169031	**84**	0	169474
11	5050	139277	**48**	70	169101	**85**	0	169474
12	4442	143719	**49**	49	169150	**86**	0	169474
13	3471	147190	**50**	44	169194	**87**	0	169474
14	2973	150163	**51**	55	169249	**88**	0	169474
15	2310	152473	**52**	32	169281	**89**	0	169474
16	2112	154585	**53**	37	169318	**90**	0	169474
17	1721	156306	**54**	36	169354	**91**	0	169474
18	1510	157816	**55**	23	169377	**92**	0	169474
19	1210	159026	**56**	21	169398	**93**	0	169474
20	1131	160157	**57**	17	169415	**94**	0	169474
21	993	161150	**58**	16	169431	**95**	0	169474
22	868	162018	**59**	6	169437	**96**	0	169474
23	762	162780	**60**	8	169445			
24	663	163443	**61**	2	169447			
25	563	164006	**62**	1	169448			
26	555	164561	**63**	1	169449			
27	454	165015	**64**	1	169450			
28	499	165514	**65**	2	169452			
29	391	165905	**66**	4	169456			
30	375	166280	**67**	0	169456			
31	349	166629	**68**	0	169456			
32	314	166943	**69**	1	169457			
33	254	167197	**70**	0	169457			
34	245	167442	**71**	1	169458			
35	202	167644	**72**	1	169459			
36	211	167855	**73**	3	169462			
37	192	168047	**74**	0	169462			

Table S3. Ipyrad assembly statistics for our total 95, subset of 34 admixed and non-admixed, and 17 non-admixed ddRADseq samples. The latter two were also included in target enrichment. Statistics are shown for loci shared across minimum 4 and 17 of the samples in our subset of 34 samples, and minimum 4 and 9 samples in our subset of 17 non-admixed individuals.

95 samples				**34 Samples**						**17 samples (non-admixed)**					
	Min4			*Min4* (~88% missing data)			*Min17* (50% missing data)			*Min4* (~23% missing data)			*Min9* (~50% missing data)		
	Total filters	Applied order	Retained loci	Total filters	Applied order	Retained loci	Total filters	Applied order	Retained loci	Total filters	Applied order	Retained loci	Total filters	Applied order	Retained loci
Total prefiltered loci	0	0	613888	0	0	78080	0	0	78080	0	0	86753	0	0	86753
Filtered by rm duplicates	9604	9604	604284	2348	2348	75732	2348	2348	75732	2251	2251	84502	2251	2251	84502
Filtered by max indels	1092	1092	603192	172	172	75560	12	12	75720	66	66	84436	11	11	84491
Filtered by max SNPs	2809	2765	600427	330	327	75233	1	1	75719	76	76	84360	0	0	84491
Filtered by max shared heterozygosity	48451	47836	552591	9820	9733	65500	304	301	75418	5514	5497	78863	159	157	84334
Filtered by min sample	383117	383117	169474	37664	37477	28023	76930	74739	679	67497	67497	11366	83588	83588	746
Total filtered loci	**445073**	**444414**	**169474**	**50334**	**50057**	**28023**	**79595**	**77401**	**679**	**75404**	**75387**	**11366**	**86009**	**86007**	**746**

Table S4. Target enrichment recovery efficiency. The table includes the number of sequenced reads and of exons recovered out of the total 536 targeted. Target length (TL). The table is organized in descending order from the sample with most loci recovered at 75% of the TL. *Marathrum* samples with relatively short exons were excluded from downstream analyses but the outgroup was included. The first sample listed is the one used for selection of sequences to be targeted with the pipeline Sondovac. Admixed individuals with the phenotype of *M. foeniculaceum* are indicates with quotation marks.

Sample	# Reads	# Exons recovered			Loci recovered
		>25% TL	>50% TL	>75% TL	
M. utile AMB497	18152507	535	535	534	208
M. utile AMB574-1	6015552	529	527	527	208
M. utile AMB503	20726495	526	526	526	208
M. foeniculaceum AMB643-1	4444374	526	526	526	208
M. foeniculaceum AMB571-1	6308716	527	526	526	208
M. utile AMB659	6645871	526	526	526	208
M. utile AMB641-1	6598011	526	525	524	208
M. utile AMB653	11275084	523	522	522	208
M. utile AMB512	4921124	525	523	522	208
M. utile AMB652	10640199	523	522	521	208
"M. foeniculaceum" AMB494	8038995	529	527	521	203
"M. foeniculaceum" AMB499	9799316	531	529	521	208
M. foeniculaceum AMB567-4	845956	524	522	520	208
M. utile AMB639-1	4951653	521	521	519	208
M. utile AMB507	843464	519	519	519	208
M. utile AMB577-3	9935840	520	519	519	208
M. foeniculaceum AMB635	4098778	522	520	518	208
"M. foeniculaceum" AMB562-1	871580	522	521	518	202
M. utile AMB577-2	15127071	519	518	517	208
"M. foeniculaceum" AMB571-4	6618910	530	527	517	203
"M. foeniculaceum" AMB502	11814928	526	524	516	203
"M. foeniculaceum" AMB561-2	2350936	528	526	516	203
M. utile AMB575-1	1971791	517	517	516	208
"M. foeniculaceum" AMB654	10076885	526	524	515	203
M. utile AMB578	9519370	516	516	515	208
M. utile AMB566-4	1589623	518	517	515	208
"M. foeniculaceum" AMB558-5	3386292	528	523	513	203
"M. foeniculaceum" AMB658-1	4293245	521	517	513	203
"M. foeniculaceum" AMB573-4	8038288	525	524	512	203
"M. foeniculaceum" AMB638-4	1878381	521	518	512	203
"M. foeniculaceum" AMB558-4	2851635	525	522	512	203
"M. foeniculaceum" AMB561-3	591426	514	513	510	203
"M. foeniculaceum" AMB657	2993130	520	516	510	203
"M. foeniculaceum" AMB506	11255969	518	513	507	203
"M. foeniculaceum" VLondono	7047222	515	512	506	208
"M. foeniculaceum" AMB555-9	507428	506	506	503	203
"M. foeniculaceum" AMB551-3	10403228	521	514	500	208
M. foeniculaceum AMB571-2	1658509	517	506	479	208
"M. foeniculaceum" AMB568	576529	498	492	478	202
M. utile AMB563-1	497235	489	484	470	206
"M. foeniculaceum" AMB556-2	447726	445	431	405	201
***M. foeniculaceum* AMB646-1**	528950	481	439	341	--
***M. utile* AMB642-1**	269227	450	387	263	--
***M. foeniculaceum* AMB632**	125422	305	204	119	--
***M. foeniculaceum* AMB645**	364733	90	60	47	--
W. squamulosa AMB513	893791	318	285	232	203

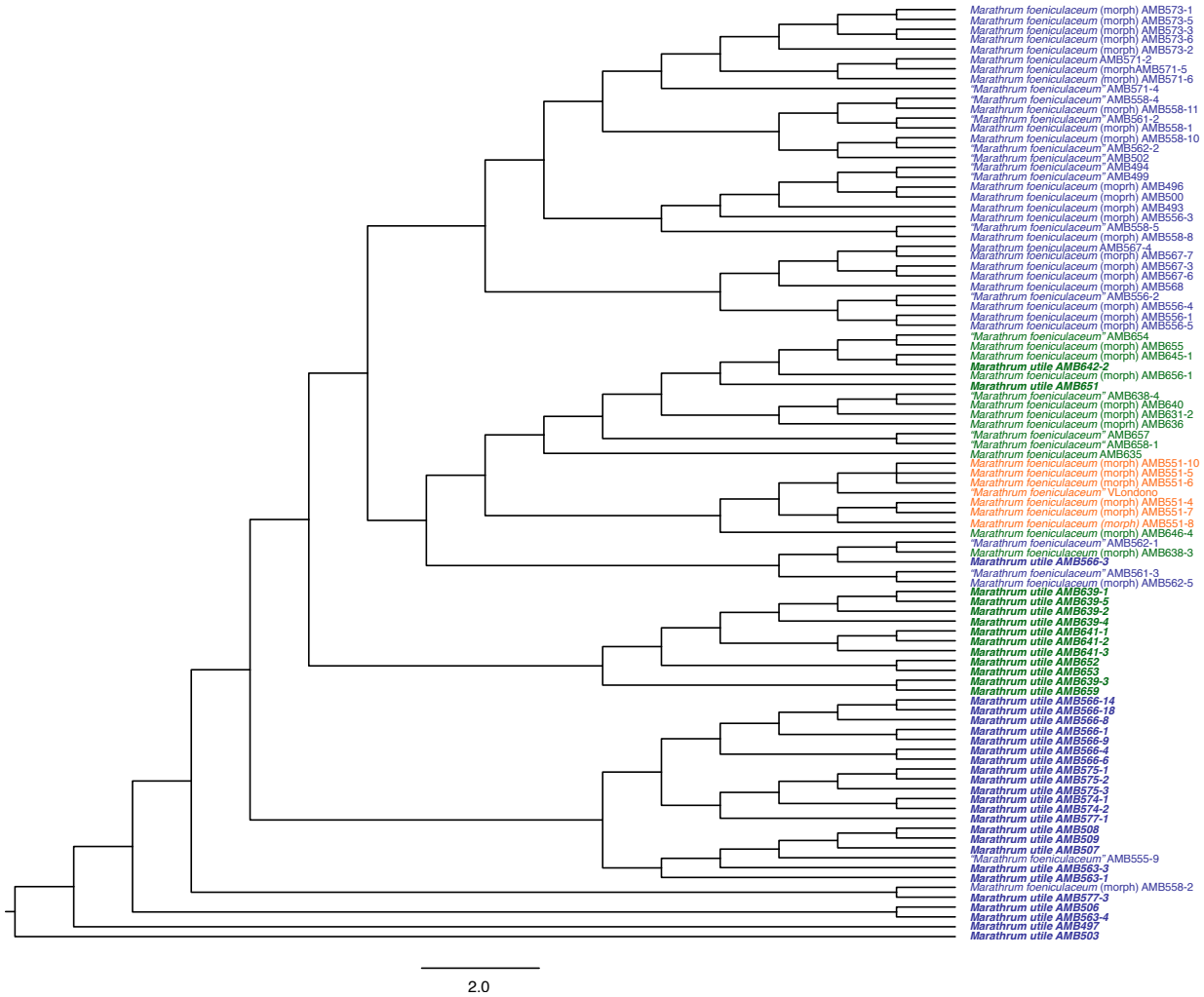

Figure S1. Species tree inferred with SVDQuartets for 95 ddRADseq samples successfully sequenced in this study. Individuals of *M. foeniculaceum* and *M. utile* (bold) from Antioquia (green), Boyacá (orange) and Caribe (blue) are shown. Tree was inferred as unrooted, but rotting is presented to be consistent with posterior analyses that were rooted with the outgroup *W. squamulosa*. Admixed individuals as inferred with ADMIXTURE are indicated with quotation marks. Individuals for which no information on genetic constitution is available but have the phenotype of *M. foeniculaceum* are indicated with "(morph)".

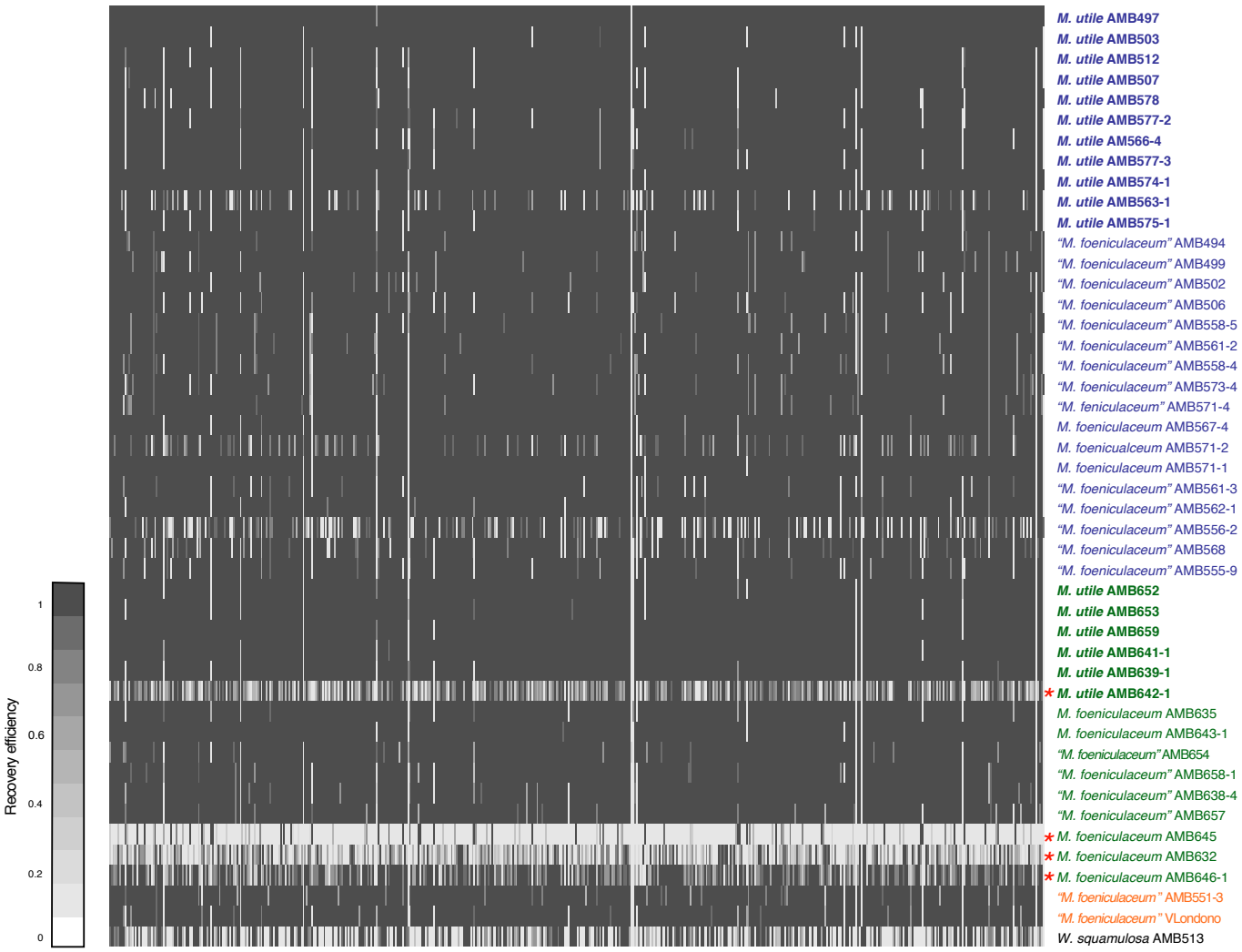

Figure S2. Target enrichment loci recovery efficiency for 42 samples (rows) across loci (columns). Recovery efficiency is measured as the length of the sequence recovered as a percentage of the length of the targeted gene. Darker gray: The full length of the targeted sequence was recovered. White: no sequence was recovered. (*) Individuals that failed sequencing or recovered short exons of low quality. Individuals of *M. foeniculaceum* and *M. utile* (bold) from Antioquia (green), Boyacá (orange) and Caribe (blue) are shown. Admixed individuals as inferred with ADMIXTURE are indicated with quotation marks.

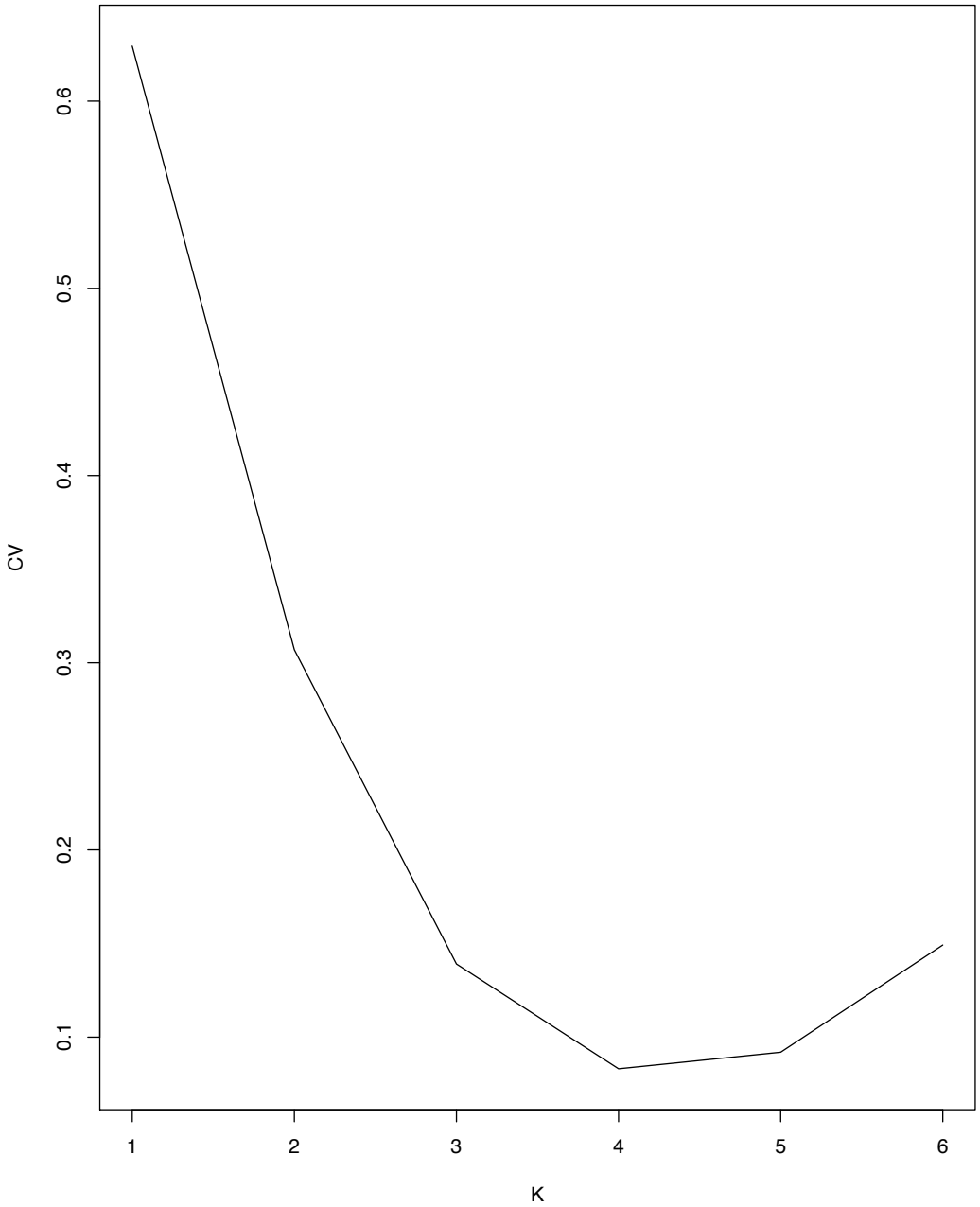

Figure S3. Cross-validation error and number of clusters (K) resulted for population genetics analysis with ADMIXTURE using target enrichment data.

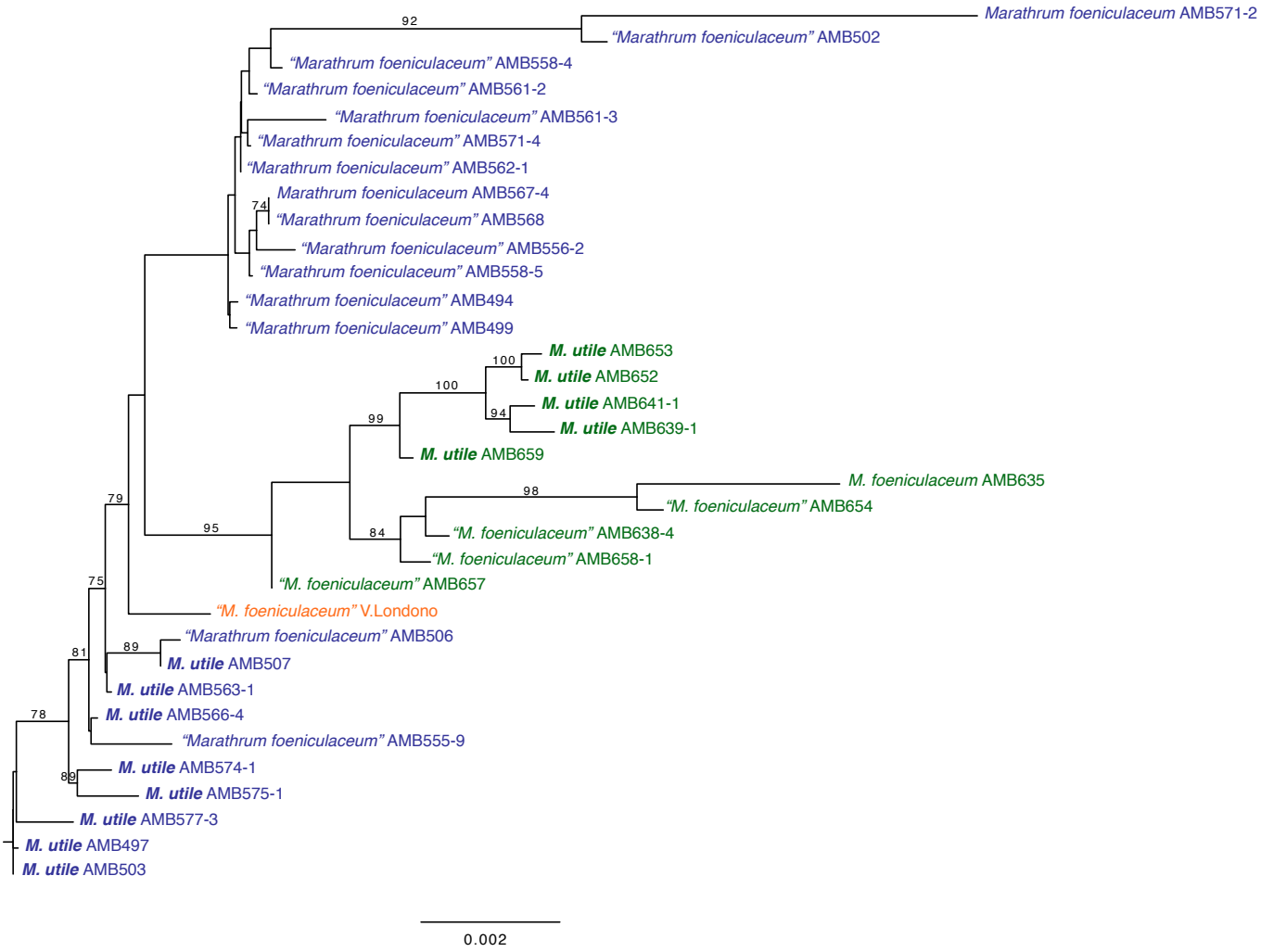

Figure S4. Maximum likelihood tree inferred from our ddRADseq dataset including only individuals that are also in the target enrichment dataset. Individuals of *M. foeniculaceum* and *M. utile* (bold) from Antioquia (green), Boyacá (orange) and Caribe (blue) are shown. Admixed individuals as inferred with ADMIXTURE are indicated with quotation marks.

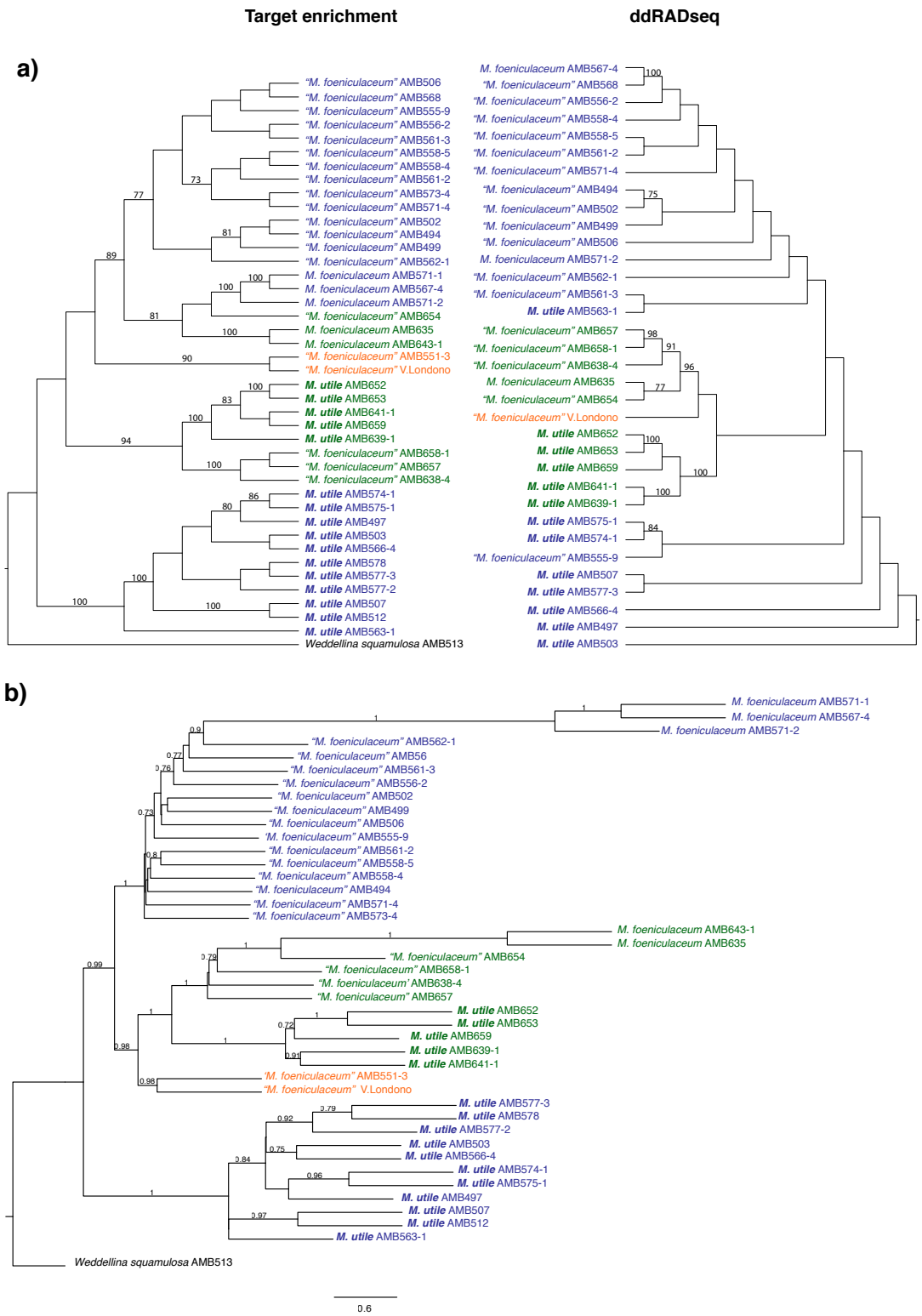

Figure S5. Species trees inferred from our target enrichment and ddRADseq data. a) SVDQuartets tree with quartet support values >70 above branches and b) ASTRAL III tree with local posterior probabilities > 0.7 shown above branches. Individuals of *M. foeniculaceum* and *M. utile* (bold) from Antioquia (green), Boyacá (orange) and Caribe (blue) are shown. Admixed individuals as inferred with ADMIXTURE are indicated with quotation marks.

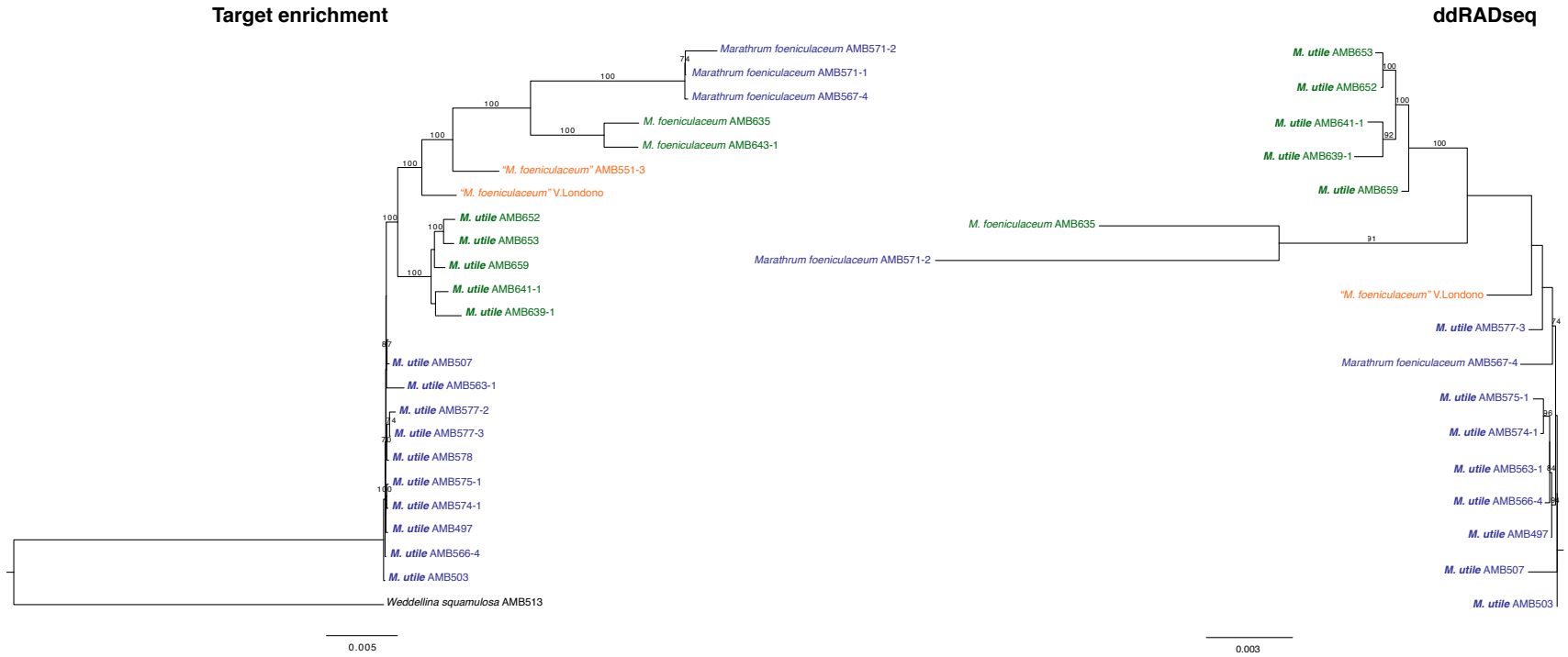

Figure S6. Maximum likelihood trees inferred from our target enrichment and ddRADseq data excluding admixed individuals from Antioquia and Caribe. Bootstrap support values >70 are show above branches. Individuals of *M. foeniculaceum* and *M. utile* (bold) from Antioquia (green), Boyacá (orange) and Caribe (blue) are shown. Admixed individuals from Boyacá are indicated with quotation marks.

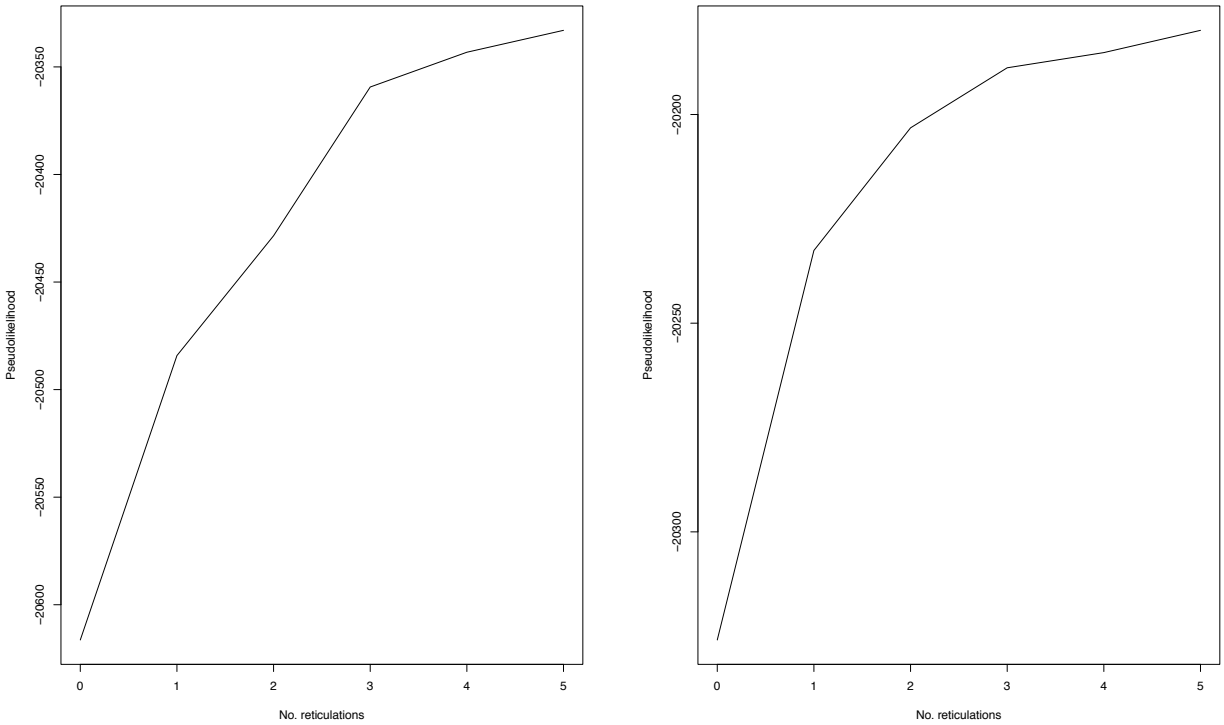

Figure S7. PhyloNet results allowing 0–5 reticulations and including admixed individuals. After 5 reticulation events, the change in pseudolikelihood score has not plateaued. Each graph represents a separate dataset with 2 semi-randomly chosen individuals per population (Antioquia, Boyacá and Caribe).